

"COLLEGE ON SOIL PHYSICS"

12 March - 6 April 2001

*Reading Material*  
(excerpt from "Soil Hydrology")

*M. Kutilek and D. R. Nielsen*

University of California, Davis  
Dept. of Land, Air and Water Resources  
Hydrologic Science  
Davis, U.S.A.

---

These notes are for internal distribution only



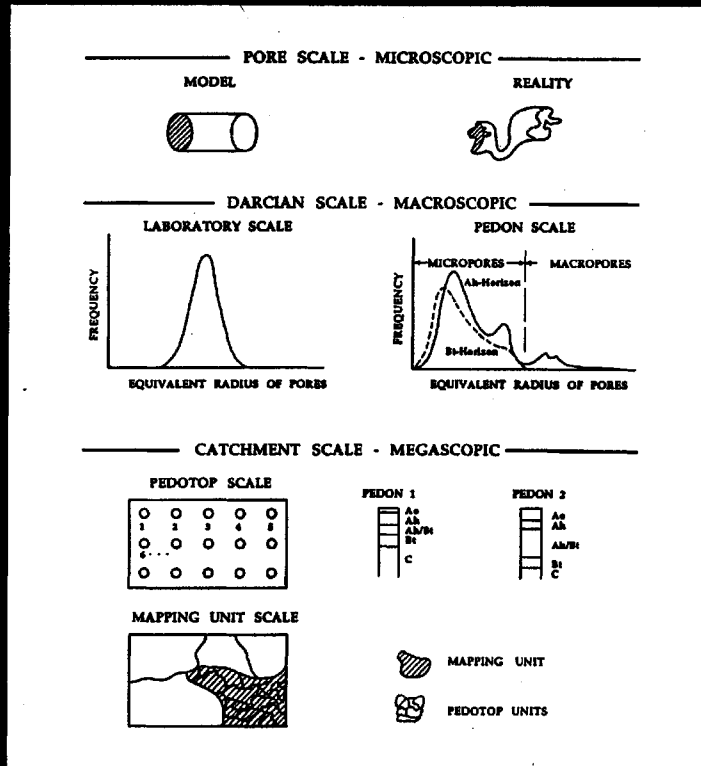
**College of Soil Physics**  
Abdus Salam International Centre for Theoretical Physics  
12 March – 6 April  
Miramare – Trieste, Italy

Reading Material  
for Lectures by

**Donald R. Nielsen**

Excerpts from  
***Soil Hydrology***  
Miroslav Kutílek and Donald R. Nielsen  
Catena-Verlag  
1994

# SOIL HYDROLOGY



## PREFACE

We have intended to present an introduction to the physical interpretation of phenomena which govern hydrological events related to soil or the upper most mantle of the earth's crust. The text is based upon our teaching and research experience. The book can serve either as the first reading for future specialists in soil physics or soil hydrology. Or, it can be a source of basic information on soil hydrology for specialists in other branches, e.g. in agronomy, ecology, environmental protection, forestry, geomorphology, hydrologic science, meteorology and water management. We assume that those specialists do not intend to conduct research in soil hydrology but they may wish to successfully use its tools in their own academic domains.

The first requirement of such a book is its simplicity without neglecting all of the complexity of soils and their porous systems as they react with the atmosphere, biosphere and hydrosphere. With mathematical derivations in the majority of cases being reduced to the level of calculus, we were obliged in some instances to deviate from the usually rigorous derivations. However, if the reader has an aversion to mathematics, basic information on any particular problem can be gained even without going into the details of its mathematical development.

According to our experience, the level of information presented in this book is adequate for a qualified use of programs and models in soil hydrology. If the reader does not intend to passively accept ready-made software, and has intentions of being more academically creative, we recommend more detailed study of information readily available in related journals and other publications.

Physical interpretation and mathematical formulation of such complex events as rain infiltration or evapotranspiration cannot be done without a certain degree of simplification. We emphasize here that this simplification leads only to an approximation to reality. Similar simplifying approaches can be applied in neighboring branches of investigation. By removing some simplifying assumptions, a more exact but usually a more complicated but still approximate solution of the soil hydrological problem is formulated.

Inasmuch as the text of our book is purposely not a monograph, the references cited are our subjective selections from the voluminous literature. Indeed, many titles to which we did not refer may be of the same importance as our selected references for a given problem. The same consideration applies to the theories presented in the text - not all are explained nor quoted in our book. Even if we had tried to subordinate our subjective choice to criteria based upon further development and broad applicability, we are aware of the fact that we would have neglected some which will eventually be extended to fundamental contributions in the future. Those contributions are the "surprises" that make research and scientific investigation so attractive to many creative brains.

For further, more detailed reading, the literature can be found in our references.

## CONTENTS

	Preface				
1	Soils in Hydrology	1			
1.1	Soils	1			
1.1.1	Soil Genesis	2			
1.1.2	Soil Classification	4			
1.1.2.1	FAO Soil Classification	5			
1.1.2.2	U.S. Soil Taxonomy	9			
1.1.3	Soil Mapping	10			
1.2	Concepts of Soil Hydrology	13			
2	Soil Porous System	16			
2.1	Soil Porosity	16			
2.2	Classification of Pores	20			
2.3	Methods of Porosity Measurement	21			
2.4	Soil Porous Systems	22			
2.5	Soil Specific Surface Problems	25 27			
3	Soil Water	28			
3.1	Soil Water Content	28			
3.2	Measurement of Soil Water Content	30			
3.2.1	Gravimetric Method	31			
3.2.2	Electrical Resistance Method	32			
3.2.3	Capacitance Methods	33			
3.2.4	Gamma Radiation Methods	37			
3.2.5	Neutron Method	39			
3.2.6	Remote Sensing Problems	43 44			
4	Soil Water Hydrostatics	45			
4.1	Interface Phenomena	45			
4.1.1	Adsorption of Water Vapor	46			
4.1.2	Capillarity	49			
4.1.3	Swelling	55			
4.2	Soil Water Potential	58			
4.2.1	Concepts of Soil Water Potential	58			
4.2.2	Units of the Potential	62			
4.2.3	Measuring Techniques	62			
4.2.3.1	Piezometers and Tensiometers	62			
4.2.3.2	Psychrometers	67			
4.2.3.3	Heat Dissipation Method	69			
4.2.4	Potential in Swelling Soils	69			
4.3	Soil Water Retention Curve	70			
4.3.1	Construction of the Soil Water Retention Curve	73			
4.3.2	Analysis of Soil Water Retention Curves	76			
4.3.3	Models of Soil Water Retention Curves Problems	79 85			
5	Hydrodynamics of Soil Water	87			
5.1	Basic Concepts	87			
5.2	Saturated Flow	88			
5.2.1	Darcy's Equation	88			
5.2.2	Saturated Hydraulic Conductivity	91			
5.2.3	Darcian and Non-Darcian Flow	97			
5.2.4	Measuring $K_s$	98			
5.3	Unsaturated Flow in Rigid Soils	102			
5.3.1	Darcy-Buckingham Equation	102			
5.3.2	Unsaturated Hydraulic Conductivity	104			
5.3.3	Richard's Equation	112			
5.3.4	Soil Water Diffusivity	116			
5.3.5	Diffusion of Water Vapor	118			
5.4	Two Phase Flow	120			
5.5	Flow in Non-rigid (Swelling) Soils	123			
5.6	Non-Isothermal Flow	124			
5.6.1	Coupled Processes	125			
5.6.2	Flow in Non-isothermal Conditions	125			
5.6.3	Flow at Temperature $T < 0^\circ\text{C}$ Problems	126 129			
6	Elementary Soil Hydrologic Processes	130			
6.1	Principles of Solutions	130			
6.2	Infiltration	133			
6.2.1	Steady Infiltration	134			
6.2.1.1	Homogeneous Soil Profile	135			
6.2.1.2	Layered Soil Profiles	136			
6.2.2	Unsteady Infiltration, Dirichlet's Boundary Condition (DBC)	140			
6.2.2.1	Characteristics of Infiltration	142			
6.2.2.2	Analytical and Semi-Analytical Procedures	144			
6.2.2.3	Approximate Solutions	153			
6.2.2.4	Empirical Equations	158			
6.2.3	Unsteady Infiltration, Neuman's Boundary Condition (NBC)	159			
6.2.3.1	Description of the Process	159			
6.2.3.2	Approximate Solutions	161			
6.2.3.3	Analytical Solutions	165			
6.2.4	Field Infiltration	166			
6.2.4.1	Soil Sealing and Crusting	166			
6.2.4.2	Infiltration into Crust- and Seal-Topped Soils	168			
6.2.4.3	Infiltration into Layered Soils	171			
6.2.4.4	Further Rainfall Infiltration Effects	173			

6.2.5	Infiltration into Seasonally Frozen Soils	174			
6.3	Soil Water Redistribution and Drainage After Infiltration	176			
6.3.1	Soil Water Redistribution after Infiltration	176	8.4	Scaling	262
6.3.2	Field Capacity	179	8.5	State-space Equations for Multiple Locations Problems	269 272
6.3.3	Drainage to the Ground Water Table	181			
6.4	Evaporation from a Bare Soil	182			
6.4.1	Steady Evaporation	183	9	Transport of Solutes in Soils	274
6.4.1.1	Homogeneous Soil Profile	183	9.1	Solute Interactions	274
6.4.1.2	Layered Soil Profiles	185	9.1.1	Molecular Diffusion	275
6.4.2	Unsteady Evaporation	187	9.1.2	Electrostatic and Electrokinetic Forces	276
6.5	Evapotranspiration	193	9.1.3	Other Reactions	278
6.5.1	Transpiration	195	9.2	Miscible Displacement in a Capillary	279
6.5.1.1	Transport of Water in Plants	195	9.2.1	Displacement without Molecular Diffusion	279
6.5.1.2	Potential and Actual Transpiration	201	9.2.2	Displacement with Molecular Diffusion	282
6.5.1.3	Wilting Point	205	9.3	Miscible Displacement in Surrogate Porous Media	284
6.5.2	Potential Evapotranspiration	206	9.3.1	Displacement in Capillary Networks	285
6.5.2.1	Computational Methods for Estimating $E_{TP}$	206	9.3.2	Miscible Displacement as a Random Walk Process	286
6.5.2.2	Structure of Evapotranspiration	209	9.3.3	Displacement in a Representative Elementary Volume	287
6.5.3	Actual Evapotranspiration $E_{TA}$	212	9.4	One-dimension Laboratory Observations	290
6.5.3.1	Soil Water Balance	214	9.4.1	Breakthrough Curves	291
6.5.3.2	Plant Surface Measurements	215	9.4.2	Magnitude of the Diffusion Coefficient	296
6.5.3.3	Micrometeorological Methods Problems	216 217	9.4.3	The Impact of Density and Viscosity	297
			9.4.4	Influences of Solution Concentration and pH	298
			9.4.5	Influence of Displacement Length	299
7	Estimating Soil Hydraulic Functions	219	9.5	Theoretical Descriptions	301
7.1	Laboratory Methods	220	9.5.1	The Convective-Diffusion Equation	301
7.1.1	Steady State Method	220	9.5.1.1	Solutes in Continual Equilibrium with the Solid Phase	305
7.1.2	Transient Methods	220	9.5.1.2	Solutes Not in Equilibrium with the Solid Phase	305
7.1.2.1	Infiltration Methods	221	9.5.1.3	Dual-Porosity Models for Structured Soils	307
7.1.2.2	Pressure Outflow Methods	221	9.5.1.4	Consecutive Convective-Diffusion Equations	309
7.1.2.3	Centrifuge Methods	223	9.5.2	Chromatographic Formulations	311
7.2	Field Methods	225	9.5.3	Stochastic Considerations	313
7.2.1	Steady Flow Methods	228	9.5.3.1	Monte Carlo Simulations	314
7.2.2	Restrictive Unsteady Flow Methods	230	9.5.3.2	Stochastic Continuum Equations	316
7.2.2.1	Infiltration Tests	230	9.5.3.3	Stochastic Convective Equations	317
7.2.2.2	Redistribution Tests	234	9.6	Implications for Water and Solute Management Problems	319 323
7.2.3	Unrestrictive Unsteady Flow Methods	237		Postscript	325
7.2.3.1	Inverse Solutions	237		Post-Postscript	333
7.2.3.2	State-Space Solutions Problems	238 243		References	334
				Index	364
8	Field Soil Heterogeneity	246			
8.1	Variability of Soil Physical Properties	246			
8.2	Concept of Soil Heterogeneity	251			
8.3	Spatial Variability and Geostatistics	252			
8.3.1	Autocorrelograms and Semivariograms	254			
8.3.2	Kriging and Cokriging	258			

## 8 FIELD SOIL HETEROGENEITY

Through their genetic development, soils are spatially variable natural bodies. Variations of parent material and vegetation across the landscape from which soils are derived influence the variability of soils even at relatively short distances. Hence, all soil properties, be they ascertained from visual observations of soil profile morphology in the field or those determined analytically in the laboratory or the field, change from one location to another. The heterogeneity of many soils within present-day mild climatic zones reflect variations of Holocene climate as well as cryoturbate features of Pleistocene glacial - interglacial periods of the Quaternary. Soil variability increases with parent material according to the sequence loess, till fluvial deposits, tectonic rocks, moraines, cryoturbates and gravity disturbates. Pedoturbation like gilgai increases variability over short distances within vertisol profiles, while soils of polygenetic character vary more in space than monogenetic soils.

We have already shown in Chapter 2 that homogeneity in soils does not exist unless we consider the concept of a representative elementary volume REV. And, if our scale of observation is less than that of the REV, the system is heterogeneous. In Chapter 2 we described REV for porosity. Other soil properties (physical, chemical and microbiological) can be treated in a similar manner. Because each soil property manifests its own REV, a value of an REV common for all kinds of observations does not exist. Generally, values of REV for capacity or static parameters differ from those for transport parameters. Moreover, values of a REV of the same property for different soils are not identical. For example, soil aggregation and the presence or absence of peds influence the value of the REV for the saturated hydraulic conductivity.

If the sampling volume is substantially increased above the REV, variations of the soil property are again evident. After briefly providing data on the variability of soil properties, we shall classify this kind of heterogeneity in relation to scale of observation.

Replicated measurements are frequently not statistically independent. In other words, soil properties measured at nearby locations vary less than those measured further apart. Because this spatial correlation impacts the results of classical statistics, the spatial variability of soils is often analyzed using regionalized variable analysis, geostatistics and applied time series analysis to identify different spatial and temporal structures within and between data sets.

Scaling techniques based upon similarity theory provide an additional opportunity to unify spatially variable field soil properties. Below we discuss statistical and scaling methods and demonstrate their practical use.

### 8.1 VARIABILITY OF SOIL PHYSICAL PROPERTIES

A table by Wilding (1985) summarizing the variability of selected soil properties expressed as a coefficient of variation is reproduced here as Table 8.1. Wilding differentiates between static soil properties (e.g. organic matter, texture, mineralogy, solum depth and soil color) and dynamic soil properties (e.g.

Table 8.1. Relative ranking of variability of soil properties that occur within landscape units of a few ha or less (Wilding, 1985).

variability of property	property
least (coefficient of variation < 15%)	soil color (hue and value) soil pH thickness of A-horizon total silt content plasticity limit
moderate (coefficient of variation 15 to 35%)	total sand content total clay content cation exchange capacity base saturation soil structure (grade and class) liquid limit depth in minimum pH calcium carbonate equivalent
most (coefficient of variation > 15%)	B2-horizon soil color (chroma) depth to mottling depth to leaching (carbonates) exchangeable H, Ca, Mg and K fine clay content organic matter content plasticity index soluble salt content hydraulic conductivity soil water content

hydraulic conductivity, soil water content, salt content, microorganisms, exchangeable cations and redox conditions). Moreover, he concludes that properties closely calibrated against a standard are less variable than those which are more qualitative (texture, color and pH versus structure, consistence and root abundance).

Based upon a large number of studies conducted during the last decade regarding spatial variability, it appears more appropriate to group soil physical properties into two classes (i) capacity parameters and (ii) transport parameters. Capacity parameters include the content of sand, silt or clay particles, organic matter content, porosity and soil water content after a sufficient period of time to remove any local perturbation caused by an event at the upper boundary of the soil profile. Such parameters usually denote static soil properties. Transport or dynamic parameters comprise hydraulic conductivity, soil water diffusivity and fluxes of water and solutes. Jury (1989) reviewing data of various authors

found that soil bulk density has the smallest variability of all soil physical characteristics with a CV generally smaller than 10%. While most values of porosity have a CV of about 10%, the variability of textural categories and the 15-bar water content is characterized by larger CV values ranging between 15 to 50%. Saturated and unsaturated hydraulic conductivity values as well as transport parameters characteristic of solute behavior are in the majority of instances well above 100%.

The variation of soil physical properties is better understood and more completely described if the probability density function (*pdf*) is estimated or ascertained. This *pdf* for an idealized normally distributed set of observations  $x$  is defined as

$$pdf = \frac{1}{\sigma\sqrt{2\pi}} \exp\left[-\frac{(x-\mu)^2}{2\sigma^2}\right] \quad (8.1)$$

where  $\mu$  is the mean and  $\sigma$  the standard deviation of the mean. For a set of  $n$  observations, the value of the *pdf* =  $N/(n\Delta x)$  where  $N$  is the number of observations of  $x$  within a class size  $[x \pm (\Delta x)/2]$ . This function is graphically demonstrated in Fig. 8.1a for 120 observations of soil water content  $\theta$ . The solid line is described by

$$N/n = \frac{\Delta\theta}{s\sqrt{2\pi}} \exp\left[-\frac{(\theta-m)^2}{2s^2}\right] \quad (8.2)$$

where  $m$  ( $= 0.433 \text{ cm}^3\cdot\text{cm}^{-3}$ ) is the estimate of  $\mu$ ,  $s$  ( $= 0.0455 \text{ cm}^3\cdot\text{cm}^{-3}$ ) the estimate of  $\sigma$  and the class  $\Delta\theta = 0.01 \text{ cm}^3\cdot\text{cm}^{-3}$ . We see that the soil water content, typical of commonly found capacity parameters, is normally distributed and manifests the well-known Gaussian or bell-shaped curve. We note that the mean as well as the median and the mode are identical and occur at the center and top of the bell-shaped curve. One half of the observations are smaller and half are larger than the median value. The mode represents the value which occurs most frequently.

When transport coefficients (e.g.  $K_s$ ,  $D$  and  $K$  for given  $\theta$  or  $h$ ) or fluxes for a given boundary condition (e.g. the infiltration rate at a particular time  $t$ ) are plotted as a *pdf*, their curves do not resemble the Gaussian shape. Inasmuch as their values vary by orders of magnitude, a Gaussian shape is sometimes manifested when they are plotted on the horizontal axis having a logarithmic scale or when their logarithmic values are plotted on the axis. Such is the case for 120 observations of hydraulic conductivity  $K$  given in Fig. 8.1b. The solid line is that of (8.2) except that  $\ln K$  has been substituted for  $\theta$  with a class of  $\Delta(\ln K) = 1$  and the other parameters calculated using the logarithmic values of  $K$ . Hence, we speak of a log-normal distribution (Nielsen et al., 1973).

A more objective test is usually used to determine if a distribution is log-normal. A better procedure consists of cumulative values of probability based upon relative number of observations plotted against the data arranged in monotonically increasing values. The cumulative probability function is

$$P\{u\} = \frac{1}{\sqrt{2\pi}} \int_{-\infty}^u \exp\left[-t^2/2\right] dt \quad (8.3)$$

where  $u = \{[g(x) - \mu]/\sigma\}$  and  $g(x)$  is the function that transforms the set of data  $x$

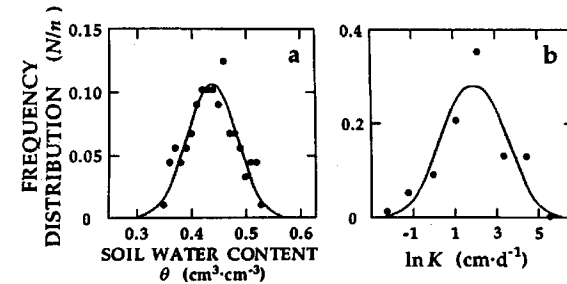


Figure 8.1. a. Probability density function of soil water content during steady infiltration manifests a normal distribution (Nielsen et al., 1973). b. Probability density function of  $\ln K$  manifests a normal distribution.

into a normal distribution. For a set of  $n$  observations, the value of  $P\{u\}$  is approximated by  $(i - 0.5)/n$  with corresponding values of  $u$  obtained from tables of  $P\{u\}$  for each observation  $i = 1, 2, 3, \dots, n$ . If we choose  $g(x) = x$  and the data fit a straight line, the values  $x$  are said to be normally distributed. If we choose  $g(x) = \ln x$  and their logarithmic values fit a straight line, the original data  $x$  are said to be log-normally distributed. In Fig. 8.2a we see that a plot of our  $K$  values is strongly curvilinear while that of  $\ln K$  is nearly a straight line. Apparently, the function  $g(x) = \ln x$  transforms our 120 values of  $K$  into a normally distributed set of observations seen in Fig. 8.2b and described by

$$N/n = \frac{\Delta K}{K s_g \sqrt{2\pi}} \exp\left\{-\frac{[g(K) - m_g]^2}{2s_g^2}\right\} \quad (8.4)$$

where  $g(K) = \ln K$ ,  $m_g = 2.28$ ,  $s_g = 1.40$  and the class  $\Delta K = 10 \text{ cm}\cdot\text{d}^{-1}$ . Unlike a normal distribution, the mode, median and mean have different values. The mode, equal to  $\exp(m_g - s_g^2)$  is  $1.39 \text{ cm}\cdot\text{d}^{-1}$ , the median, equal to  $\exp(m_g)$  is  $9.74 \text{ cm}\cdot\text{d}^{-1}$  and the mean, equal to  $\exp(m_g + 0.5s_g^2)$  is  $25.79 \text{ cm}\cdot\text{d}^{-1}$ . For a log-normal distribution, we note that only a few very large values yield a mean value substantially larger than that of the majority of the observations. Not recognizing that the observed values of  $K$  were not log-normally distributed would cause the mean to be underestimated by about 20%  $\{[25.79 - 20.63]/25.79\}$  where the arithmetic mean is  $20.63 \text{ cm}\cdot\text{d}^{-1}$ .

A still better procedure for ascertaining the type of *pdf* involves the Kolgomorov-Smirnov test or the  $\chi^2$  test. However, no test is considered an absolute proof regarding the type of *pdf*. In addition to normal and log-normal distributions, many other types of *pdf* such as the Weibull, Gamma or Erlang functions can be advantageously used to fit sets of sampled data.

When a property  $A$  is studied, an observational sample of  $A$  is the estimate  $(A + \epsilon)$  where  $\epsilon$  is the error of the measuring method. The real *pdf* of  $A$

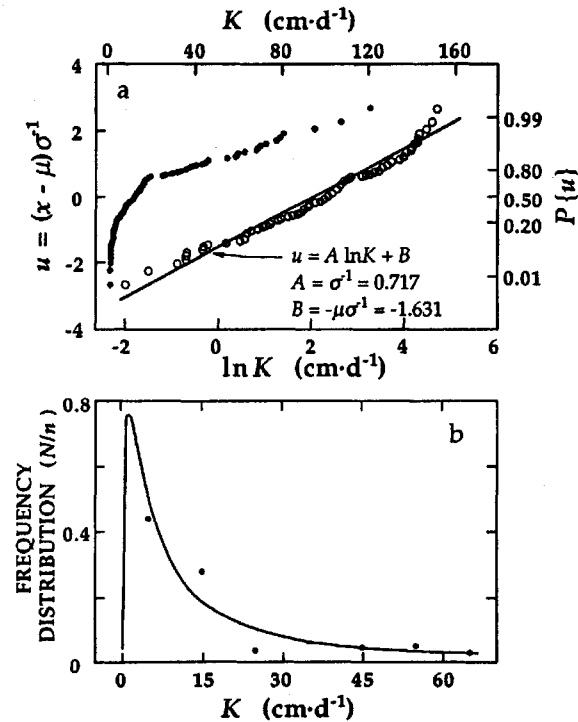


Figure 8.2. a. Fractile diagram of  $K$  and  $\ln K$ . b. Probability density function of  $K$  manifests a log-normal distribution described by (8.4).

is not necessarily equal to the *pdf* of  $(A + \epsilon)$ . Thus, the error of various experimental methods deforms our observation of  $A$ . For example, if  $K_S$  is determined by three different methods and if by each method we obtained the subset of  $K_S$  of the same population, we can compare the *pdf* of the subsets. When *pdf* are of the same type only for two different methods, only those estimates of  $K_S$  are mutually compatible.

## 8.2 CONCEPT OF SOIL HETEROGENEITY

Soil heterogeneity will be discussed with the aim of a realistic description of soil hydrological processes. Soil heterogeneity can have either stochastic or deterministic character. Stochastic heterogeneity concerns soils with randomly variable properties defined as a realization of a random function studied through observation and data sampling. The realization is unique and deterministic but unknown to us.

Deterministic heterogeneity is related to our knowledge regarding a distinct change of soil properties, as e.g. the existence of layers within a profile or boundaries between soil districts. With a distinct change of a soil taxon we expect a change of soil physical properties. Two neighboring taxons, each characterized in space by randomly varying hydraulic properties, are distinguishable if the first and second moments for each taxon are spatially distinct. One of the aims of statistics is to confirm this distance and to objectively define the boundary between the two taxons if such a boundary even exists. Hence, we use statistics to quantify soil hydraulic characteristics which are deterministically related to pedological characteristics. These hydraulic properties characterizing districts of pedotaxons are frequently given on soil maps. In each of the districts, random heterogeneity exists. Hence, a mosaic of deterministic districts each manifesting random heterogeneity comprises soil maps. We assume the links between hydraulic and pedological properties may be complemented by geomorphological and geobotanical features.

For field soil hydrology we start with the *macroscopic* or *Darcian scale* which for field conditions is related to the pedon, and therefore we speak of a pedon scale. Its size is determined by the REV related to transport characteristics, mainly  $K_S$ . Such observations for the solution field problems are frequently called "point" data. In relation to soil survey, pedon is considered a homogeneous unit having a size of about  $10^0 \text{ m}^2$ .

On the farmer's field we frequently deal with a set of pedons belonging to the district of the lowest taxonomic unit - pedotop described as a family or soil series. The stochastic character of soil heterogeneity of such an areal unit having a size of about  $10^4 \text{ m}^2$  and possibly much more is included in the *soil series* (or *pedotop*) scale. Examples of variability at this scale were shown in section 8.1.

On the *watershed* or *regional scale*, the lowest pedotaxons are clustered to soil mapping units of higher pedotops. At this realistic megascale, objective, comprehensive studies of water and solute fluxes have yet to be experimentally measured in the field. A surrogate analysis is presently provided by introducing pedotransfer functions which relate soil hydraulic functions to basic and simply measured soil data such as the content of clay, silt, sand, organic matter and values of bulk density or porosity. Although those functions obtained by regression analyses can not replace direct measurements and estimates of soil physical properties [e.g.  $K_S$  or  $h(\theta)$ ], they can improve interpolation between field experimental points, i.e. to extend pedon-size data to entire pedological districts. In the remainder of this chapter, we deal primarily with the soil series scale (pedotop scale).

### 8.3 SPATIAL VARIABILITY AND GEOSTATISTICS

Soils vary continuously in space, especially when we consider domains at the soil series scale. However, our measurements of soil physical properties yield sets of discrete values for particular "point" locations within our soil sampling area. For a more complete interpretation of those discrete measurements, the theory of regionalized variables transforms our point discrete data to the soil continuum.

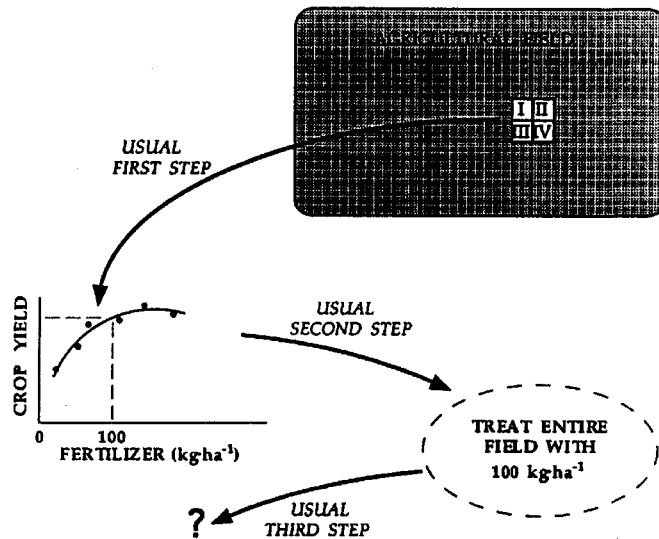


Figure 8.3. Small, replicated plot scheme typical of agricultural research.

Achievements in agricultural production have been aided by small, replicated plots established on sites believed to be "typical" or "representative" of a farmer's field or an agricultural landscape. Crop responses on these small plots treated with fertilizers, pesticides, irrigations, etc. were interpreted and formed the basis for uniformly treating an entire field. Figure 8.3 illustrates the all-too-common method today of conducting agronomic field research. In an agricultural field an experiment is located at a site which is assumed to be "representative" of the rest of the field as well as the soil of the agricultural region. With replicated treatments established in four statistical blocks, the first step is to establish the regression between crop yield and treatment. In this

example, a maximum yield is measured at about  $150 \text{ kg}\cdot\text{ha}^{-1}$  fertilizer. Being mindful of the desire not to waste fertilizer or pollute the subsoil environment with excess fertilizer and also noting that  $100 \text{ kg}\cdot\text{ha}^{-1}$  fertilizer produced a yield close to the maximum, the second step is a recommendation to apply  $100 \text{ kg}\cdot\text{ha}^{-1}$  fertilizer over the entire field. With an increased yield being obtained when the recommendation is followed, the farmer is happy. What is the usual third step taken in the above experimentation? It varies from repeating the same experiment or modifying its treatment levels, going to another field or soil condition or doing nothing more. Doing nothing more does not benefit the farmer nor does it benefit agriculture or the environment. Another sampling across the entire field could detect specific locations within the field where, for example, crop production could be increased, excessive levels of the fertilizer nutrient and deficiencies of other plant nutrients prevail or changes in soil quality indicative of achieving or denying sustainable agriculture are observed. Yes, another sampling across the entire field would ascertain if the farmer could make still further improvements in crop and soil management without necessarily imposing different treatments in still another replicated small plot experiment. Similar inefficient procedures can be found in research and in practical applications of soil hydrology.

Assuming steady-state conditions, deterministic concepts and mass balance equations have usually been applied for relatively short time periods – minutes, days, weeks or for times no longer than a growing season. Attempts to assess the impacts of agricultural methods and weather events between and during several growing seasons have been made through long-term experimental plots managed for decades, and in a few cases for more than a century. These kinds of experiments remain effective today when one wishes to ascertain the effect of a particular treatment relative to crop or animal production. On the other hand, they do little for improving our understanding of how agricultural practices impact on the quality of water leaving a cultivated field or rangeland. Moreover, they provide no direct information regarding the all-too-often subtle changes in soil quality occurring on a farm or within an agricultural region.

During the century, we have asked the question, "Does the treatment cause a significant perturbation from the expected mean?" We have used analysis of variance and regression techniques designed to minimize the impact of spatial or temporal heterogeneity in field soils and until recently, have not even taken the time to record where we take an observation within an experimental plot or field.

Regionalized variable analysis considers the distance between pairs of measured values as the main criterion in dealing with the variance. Here lies one of the main differences between classical "Fisher" statistics and geostatistics. Whereas the coordinate system is ignored in classical "Fisher" statistics, it is used in geostatistics to better answer the question, "How far apart should we take our samples?"

8.3.1 Autocorrelograms and Semivariograms

A geostatistical evaluation of data is performed using two tools; (i) the autocorrelogram and (ii) the semivariogram. Both tools can be used for data obtained in 1, 2 and 3 dimensions as well as in time. For the sake of simplicity here, we limit our description and their construction for sampling along a transect at regular intervals.

For an explanation of an autocorrelogram, we consider a transect of equidistant sampling and measurements of soil property  $A$ . We obtain a value of  $A$  at location  $x_1$  designated as  $A_1(x_1)$ , and similarly  $A_2(x_2), A_3(x_3) \dots A_n(x_n)$ , see Fig. 8.4. We compute correlation coefficients for pairs separated by a specified distance  $h$  using the relation

$$r(h) = \frac{\text{cov}[A(x), A(x+h)]}{\sqrt{\text{Var}[A(x)]}\sqrt{\text{Var}[A(x+h)]}} \tag{8.5}$$

For example, if we specify a distance  $h = 0$ , we find for pairs  $[A(x_i), A(x_i)]$  a correlation coefficient  $r_0 = 1$ . For pairs  $[A(x_i), A(x_{i+1})]$  at a distance  $h = 1$  (nearest neighbors), we obtain a value of  $r_1$ . Next, we increase the distance between the neighbors to  $h = 2$  for pairs  $[A(x_i), A(x_{i+2})]$  and obtain a value for  $r_2$  and so on. Details of the calculation are e.g. Webster, 1985; Webster and Oliver, 1990. Finally, we plot  $r_i$  versus  $h$  or  $r(h)$  and we obtain the function illustrated in Fig. 8.4. The distance between neighbors  $h$  is called the lag. The distance over which

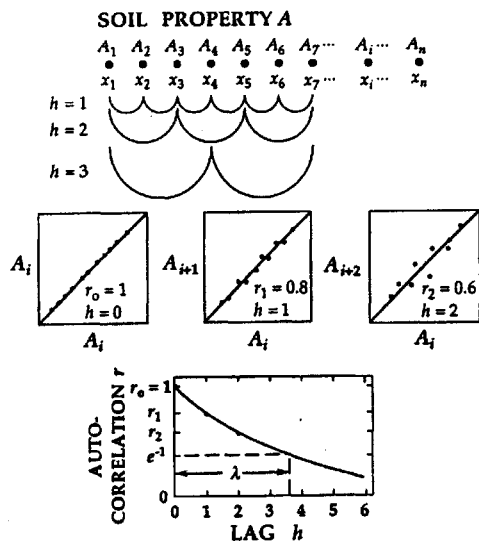


Figure 8.4. Derivation of the autocorrelogram with equidistant sampling along a transect.

a significant correlation exists is called the correlation length, scale, or range. Commonly, the correlation length  $\lambda$  is defined for a 1-dimensional transect by the relation

$$r = r_0 \exp(-x / \lambda) \tag{8.6}$$

where the value of  $r_0 = 1$  and that of  $r$  is diminished to  $e^{-1}$  at a distance of  $\lambda$ . Figure 8.5a presents soil water content  $\theta$  measured in a field at 1-m intervals with a neutron moisture meter at the 50-cm soil depth within a 160-m long transect. Neglecting the locations of the observations ( $n = 160$ ), the mean  $m$  and standard deviation  $s$  of the 160 observations are  $0.136$  and  $0.0162 \text{ cm}^3\text{-cm}^{-3}$ , respectively. Figure 8.5b, the autocorrelogram of the 160 observations, shows that the autocorrelation length  $\lambda$  is about 6 m. Sampling at intervals less than 6 m is somewhat unnecessary because the observations are related to each other. Sampling at intervals greater than 6 m does not allow meaningful interpolation between neighboring observations. It should be obvious that the functional relation between  $r$  and  $h$  depends upon the size of the sample, and that in general, the greater the sample size, the greater the value of the autocorrelation length  $\lambda$ .

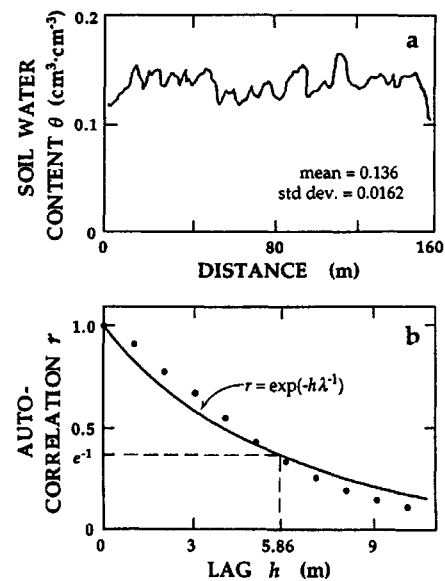


Figure 8.5. a. Values of soil water content  $\theta$  measured with a neutron probe along a 160-m transect at 1-m intervals. b. Autocorrelogram of  $\theta$  illustrating a correlation length  $\lambda$  of 5.86 m.

When we calibrate a soil moisture meter, we should try to sample at distances smaller than the value of  $\lambda$ . Or, when  $K_S$  is measured on samples of various sizes, autocorrelograms for each size provide estimates of  $\lambda$ . As the size of the sample increases, the value of  $\lambda$  or the scale of the autocorrelogram approaches an upper limit which defines the value of the REV. The same technique can be used to ascertain the magnitude of the REV of  $\theta$  for a particular value of  $h$ . Or by using different sampling volumes, we can establish equal autocorrelation scales for both  $\theta$  and solute content when we formulate transport equations for leaching.

The concept of autocorrelation is applicable only if second order stationarity exists, i.e. if the variance is constant across the field. Spatial trends across fields or within soil profiles can be found from autocorrelation functions. If there are shoulders within  $r(h)$  or if  $r(h)$  remains large as the separation distance increases, we can assume that trends exist. Because nonlinear trends yield different correlation scales for different sampling grid densities, trends along a transect can be examined by a regular dropping out of data to change the density of sampling. The correlation scale is also probably interrelated with transect spacing (Jury, 1989).

The concept of variance known from classical statistics is extended in geostatistics to consider the location of the observations  $[A(x_i), A(x_i + h)]$  separated by a distance  $h$ . The equation for the construction of the semivariogram is

$$\gamma(h) = \frac{1}{2n} \sum_{i=1}^n [A(x_i+h) - A(x_i)]^2 \quad (8.7)$$

As the distance between pairs of observations or lag  $h$  increases,  $\gamma(h)$  rises and asymptotically approaches the value of the variance called the sill, see Fig. 8.6. The sill is approached at  $h = \lambda$  denoted as the range or scale of the variogram as well as the zone of correlation. For  $h < \lambda$ , the variance is deformed by the position of the sampling points, or in other words, by the spatial dependence otherwise called the spatial structure. Methods for calculating  $\lambda$  are reviewed by Peck (1984). Semivariograms for spatially independent and dependent data as well as for a spatially changing domain are illustrated in Fig. 8.6. If the domain is spatially changing and not statistically homogeneous,  $\gamma(h)$  increases and does not approach a sill. Methods for dealing with this situation are described in the literature (e.g. Webster, 1985). The intercept at  $h = 0$  is called the nugget and usually appears as a consequence of fine scale estimates not being available. The nugget also includes the measurement error. Uehara et al. (1985) collected surface soil samples on a 1-km grid within a single soil series in Sudan extending over an area of about 400 km<sup>2</sup>. Additional samples only 1 m apart were also collected. Each sample was analyzed for exchangeable sodium percentage inasmuch as that soil attribute was judged to be most likely to limit sugarcane production. The spatial variance structure of the exchangeable sodium percentage across the domain is apparent in Fig. 8.7. The variogram has a nugget of 6.15, a range of 3 km and a sill and sample variance of 21.6. Kriged contours of exchangeable sodium percentage having values between 5 and 21% had a mean estimation variance of 10.5. (Kriging and co-kriging are discussed in the next section.)

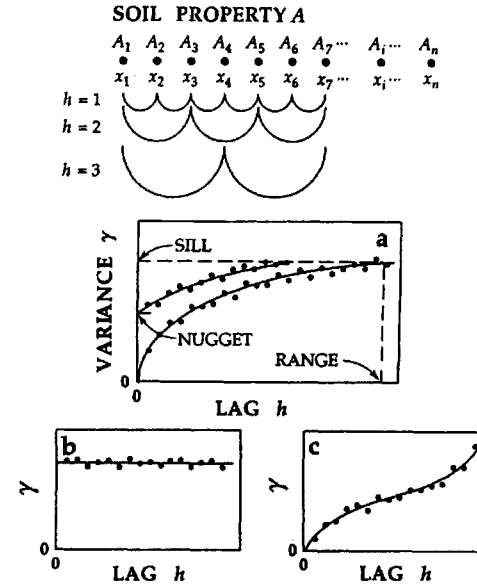


Figure 8.6. Derivation of the semivariogram with equidistant sampling along a transect: a. spatially dependent with and without a nugget, b. spatially independent and c. spatially changing domain.

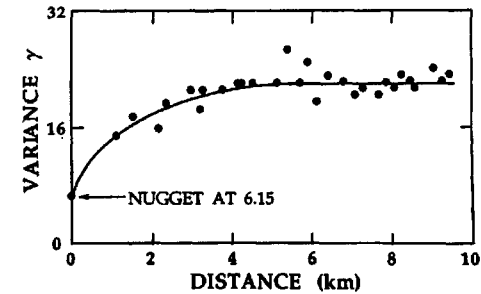


Figure 8.7. Semivariogram of exchangeable sodium percentage from samples taken on a 1-km grid over a 400-km<sup>2</sup> area of a mapping unit in Sudan (Uehara et al., 1985).

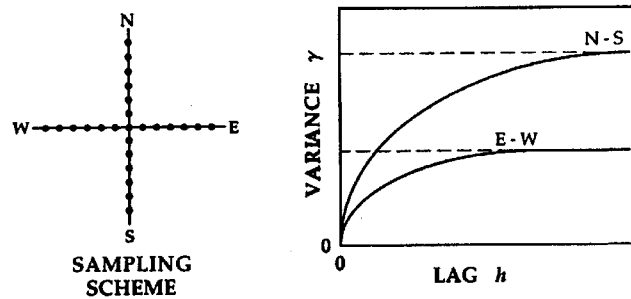


Figure 8.8. Semivariograms of two perpendicular transects of a non-isotropic domain.

In a non-isotropic domain variograms differ for different directions, see Fig. 8.8. For sampling on a rectangular grid, constructing variograms along the main two directions of the grid and on the two diagonals is a logical first choice to identify the presence of non-isotropic behavior. For the construction of the appropriate semivariograms, computed data  $\gamma(h)$  are fitted to a simple curve, usually the segment of a circle, or that of an exponential or hyperbolic curve. Interpreting semivariograms is made somewhat more reliable if a couple of "rules of thumbs" are followed. First, the minimum number of samples along a transect should be in the range of 50 to 100 (Gutjahr, 1985; and Webster, 1985). And second, the estimation of  $\gamma(h)$  is considered reliable for lags not exceeding 20% of the total transect length.

The term support refers to the size, shape and orientation of samples. An increase of support, called regularization, generally leads to a decrease of variation.

Reviewing data of various authors, Jury (1989) shows that the correlation length  $\lambda$  of a given soil property varies significantly. In some instances when the value of  $\lambda$  depends upon the sample spacing along the transect, we deal with a scale effect. In such cases, several theories provide an explanation (e.g. a violation of the stationarity hypothesis).

### 8.3.2 Kriging and Cokriging

Derived information on spatial variability in the form of  $r(h)$  and  $\gamma(h)$  can be advantageously used for estimating a soil property at locations where it is not measured. Kriging is a weighted interpolation named after D. G. Krige (1966) who devised it for estimating the gold content of ore in South Africa. Although its theoretical foundation was apparently recognized much earlier (Kolmogorov, 1941), its present day development is largely attributed to

Matheron (1965) and his associates. If  $A(x_1)$  and  $A(x_2)$  are measured values of  $A$  at locations  $x_1$  and  $x_2$ , respectively, we seek an unbiased estimate of  $A$  in between  $x_1$  and  $x_2$ . We interpolate with weights  $\mu$  and  $\nu$  for each of the positions  $x_1$  and  $x_2$ . Values of  $\mu$  and  $\nu$  depend upon the covariance function or the semivariogram as well as upon the location of the interpolated value. Note that the weights do not depend upon the actual values of  $A$ . The kriging variance or the minimum square error  $\sigma_k^2$  is a measure of the precision of the interpolated value. Many kriging formulations are available (e.g. Journel and Huijbregts, 1978). Here, we briefly introduce punctual kriging.

For  $n$  sampling points  $x_i$  ( $i = 1, 2, \dots, n$ ) in a field,  $A$  is estimated (or kriged) at  $x_0$  by

$$A^*(x_0) = \sum_{i=1}^n \lambda_i A(x_i) \quad (8.8)$$

where  $\lambda_i$  are the weights assigned to the sampling points and have a sum of unity. The kriging variance is

$$\sigma_k^2(x_0) = 2 \sum_{i=1}^n \lambda_i \bar{\gamma}(x_i, x_0) - \sum_{i=1}^n \sum_{j=1}^n \lambda_i \lambda_j \gamma(x_i, x_j) - \bar{\gamma}(x_0, x_0) \quad (8.9)$$

where  $\gamma(x_i, x_j)$  is the semivariance of  $A$  between the  $i$ th and  $j$ th sampling points,  $\bar{\gamma}(x_i, x_0)$  is the average semivariance between the  $i$ th sampling point and the field and  $\bar{\gamma}(x_0, x_0)$  is the average variance within the field. The kriging variance is least when

$$\sum_{i=1}^n \lambda_i \gamma(x_i, x_j) + \mu_L = \bar{\gamma}(x_j, x_0) \quad (8.10)$$

for all  $j$  where  $\mu_L$  is the Lagrange multiplier. The solution of (8.10) subject to the sum of the weights  $\lambda_i$  being unity provides values of the weights  $\lambda_i$  used in (8.8) as well as that of  $\mu_L$ . These values also allow estimation of  $\sigma_k^2(x_0)$  with

$$\sigma_k^2(x_0) = \sum_{i=1}^n \lambda_i \bar{\gamma}(x_i, x_0) - \bar{\gamma}(x_0, x_0) + \mu_L \quad (8.11)$$

An example of kriging along a transect is given in Fig. 8.9. With kriging, additional optimal locations of sampling can be gained inasmuch as the kriged isolines depict more objectively the district of soils than an interpolation done by eye, or by linear interpolation between the measured data. The results of kriging depend upon the fitted semivariogram and can be easily validated as follows. An estimate of  $A$  is made for each location  $x_j$  for which an observation was obtained but is purposely left out of the kriging process. The procedure ("jack-knifing") is repeated for each of the measured  $j$  locations. The differences between the kriged and observed values are related to  $\sigma^2$ , and if equal to 1, the kriging procedure has been properly executed. The computational procedure is readily available in the literature (e.g. Journel and Huijbregts, 1978; and Webster, 1985).

In the derivation of the autocorrelogram we considered the spatial correlation of only one soil property with itself - hence, the term autocorrelation. The same principle can be applied to two properties  $A$  and  $B$  to determine to what extent property  $A$  at location  $x_i$  depends upon  $B$  at  $x_{i+1}$ . Here,

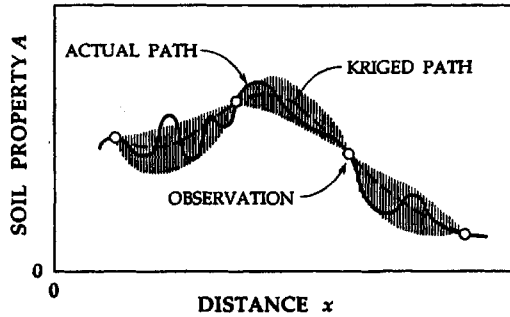


Figure 8.9. Demonstration of Kriged estimates yielding a smoother path than the actual path (Gutjahr, 1985). The shaded area represents  $\pm\sigma_k$ .

we deal with random fields of two properties, and when we transfer spatial variability information from one field to the other, their variables are co-regionalized or cross-correlated. The procedure is particularly useful when sampling locations for variable A are not identical to those for variable B, e.g. variable B is more densely sampled than variable A. Practical considerations of cost of analysis, reliability of particular measurement procedures, ease and access of sampling locations and time all contribute to the numbers of observations selected. For example, the available water content AWC in a soil profile and soil water content at  $pF = 2.5$  are more difficult and expensive than the contents of sand, silt and clay. The semivariogram of these five properties and their cross-semivariograms are plotted in Fig. 8.10 and used in co-kriging procedures to obtain the contour isarithmic maps given in Fig. 8.11. The detailed computational procedure is described by Vauclin et al. (1983).

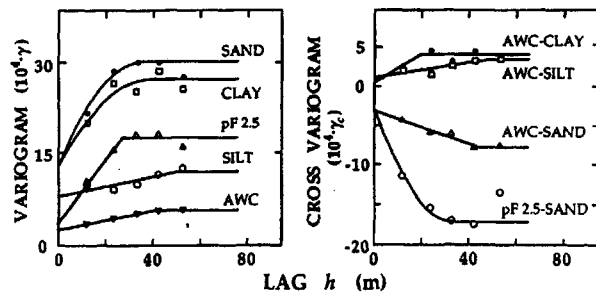
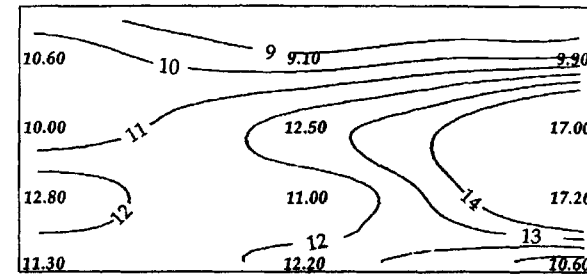


Figure 8.10. a. Semivariograms of five soil physical properties and b. Cross-semivariograms. AWC is available water content and  $pF 2.5$  represents the soil water content at  $pF = 2.5$ .



10.99	10.70	10.42	9.90	10.09	10.23	10.36	11.02	11.19
10.81	10.47	10.09	10.14	10.23	10.42	10.63	11.08	12.25
10.60	10.32	10.35	10.37	9.10	10.72	10.99	11.28	9.90
10.55	10.53	10.53	10.65	10	10.82	11.48	11.41	11.88
10.65	10.63	10.75	10.97	11.24	11.56	11.91	12.87	12.93
10.75	10.93	11.18	11.28	11.82	11.98	12.72	13.27	13.72
10.00	11.09	11.38	11.73	12.50	12.65	13.23	13.87	17.00
11.12	11.17	11.56	12.09	12.59	12.96	13.58	14.20	14.59
11.99	11.40	11.75	12.28	12.74	13.34	13.99	14.29	14.68
11.63	11.66	11.95	12.39	12.76	13.40	13.98	14.37	14.73
12.80	11.89	12.00	12.16	11.00	12.08	13.63	14.22	17.20
11.79	11.90	12.04	12.20	12.33	12.85	13.29	13.76	14.13
11.79	11.87	12.03	12.11	12.24	12.45	12.91	13.23	13.51
11.64	11.67	11.89	12.00	12.12	12.26	12.48	12.67	12.88
11.30	11.62	11.77	11.88	12.20	12.08	12.17	12.22	10.60

10.77	10.39	9.75	9.62	9.07	9.96	10.12	10.75	10.70
10.68	10.21	9.85	9.90	9.90	10.31	10.50	10.84	10.78
10.60	10.16	10.24	10.30	9.10	10.77	11.01	10.95	9.90
10.37	10.62	10.58	10.60	10	10.91	11.73	11.58	11.75
9.76	10.56	11.60	11.06	11.25	11.96	14.02	12.88	10.90
10.53	10.67	11.03	11.26	11.77	12.30	12.94	13.84	13.97
10.00	10.71	10.40	11.40	12.50	12.63	13.20	13.78	17.00
10.72	10.79	11.04	11.55	12.34	12.82	13.41	14.01	14.38
10.60	11.07	10.63	11.58	11.36	13.11	13.74	14.14	14.42
11.47	11.70	12.00	12.20	12.52	13.29	13.69	14.18	14.66
12.80	12.10	13.62	12.96	11.00	13.05	13.65	14.29	17.20
12.80	12.06	12.20	12.40	12.42	12.83	13.77	13.83	14.25
12.80	11.94	11.15	12.03	12.44	12.44	12.27	13.78	14.30
11.76	11.57	11.65	11.85	12.08	12.20	12.48	12.75	13.04
11.30	11.44	11.02	11.71	12.20	12.05	12.44	12.32	10.60

Figure 8.11. Isolines of available water content using data from Fig. 8.10 (top fig.). The accuracy of the map increases when kriging is used (middle fig.) and co-kriging is used (bottom fig.). The bold, horizontal numbers correspond to measured values (Vauclin et al., 1983).

## 9 TRANSPORT OF SOLUTES IN SOILS

In Chapter 3 we acknowledged that the liquid phase of a soil is never just pure water, and in Chapter 4 and subsequent chapters we rigorously defined soil water potential to include consideration of the quantity and diversity of solute species in the soil solution. Nevertheless, up to now, we did not consider the physical, chemical and biological processes within a soil profile that distribute, dilute or concentrate solute species within the liquid phase of a soil. Inasmuch as the relative concentration of solutes in the liquid phase governs not only the retention and transport of water within soils but also contributes to our understanding of managing the quality of water within soils as well as that moving below the recall of plant roots deeper into the vadose zone, we present here both microscopic and macroscopic considerations of solute behavior in soils. We limit our discussion to the soil solution and consider transport in the soil air only when it plays an important part in transport of the soil solution.

Although it has been known for at least a century that water and solutes do not travel uniformly within field soils (Lawes et al., 1881), relatively few soil hydrologists individually or collectively made a concerted effort to study and understand the topic until recent times. A few studies now considered classic kept the topic alive until the 1950s. In 1900, Means and Holmes (1901) provided a lucid description of the chemical and physical processes occurring within soils during and after rainfall and irrigation events. They understood the complexities of molecular diffusion and convection in a reactive, structured soil manifesting a heterogeneous pore size distribution. Later, Slichter (1905) noted of a water soluble chemical or "tracer" added to ground water, "its appearance ... is gradual" when measured at a downstream well. He explained that the gradual appearance of the tracer was caused by the fact that the central thread of water in each capillary pore of the soil moves faster than the water along the walls of the pore. Thirty years later, Kitagawa (1934) studying the dispersion of sodium chloride from a point source in a water-saturated sand expressed the mixing process as a function of the average pore water velocity. Approximately 10 and 20 years later, Bosworth (1948) and Taylor (1953) examined the contributions of molecular diffusion in cylindrical capillary tubes. During the succeeding forty years, investigations have accelerated owing to the growing importance of water quality. In this chapter we limit our discussion to miscible displacement - that is, when two miscible fluids are brought into contact, the initial abrupt interface between the two becomes blurred. The abrupt interface disappears owing to a mixing process dependent upon the properties of the two fluids, the properties of the porous medium, the nature of the microscopic velocity distributions of the fluids and the reactions occurring within each fluid as well as between each fluid and the porous medium.

### 9.1 SOLUTE INTERACTIONS

We consider here those physical interactions of solutes that play a primary role in the distribution of solutes within the soil profile.

#### 9.1.1 Molecular Diffusion

Thermal energy provides a continual, never ending movement of gas and liquid phases of a soil system. In 1855, Fick provided a theoretical basis for this movement by showing that molecular diffusion obeyed the same mathematical laws that Newton had derived for momentum flux and Fourier for heat flux. The solid matrix of the soil complicates matters by altering both the diffusion path length and the cross sectional area available for diffusion as well as providing an electric field and reactive surfaces that further alter molecular movement.

Fick's first law of diffusion states that a gaseous or solute species moves or diffuses relative to a mixture or solution in the direction of decreasing concentration of that species just as heat flows by conduction in the direction of decreasing temperature. Hence,

$$q = -DA \frac{dC}{dx} \quad (9.1)$$

where  $q$  is the diffusive flux [ $MT^{-1}$ ],  $A$  the cross sectional area [ $L^2$ ],  $C$  the concentration [ $ML^{-3}$ ],  $x$  the space coordinate [ $L$ ] and  $D$  the molecular coefficient [ $L^2T^{-1}$ ]. Because concentration in a porous medium can be expressed in a number of ways,  $C$  should be of the same quantity reference as  $q$ , and the volume should be of the same length reference as  $x$  and  $A$ . Jackson et al. (1963) provide details for expressing the frame of reference as the entire bulk soil system or either one of the two fluid phases. Temperature gradients, pressure gradients and external forces also contribute to the diffusive flux. Gaseous diffusion coefficients in soil air are almost composition independent, increase with temperature and vary inversely with pressure. Coefficients in soil water depend upon concentration, solute species and usually increase with temperature. Comprehensive treatments of molecular diffusion are available (e. g. Bird et al., 1960; Crank, 1956; and Currie, 1960).

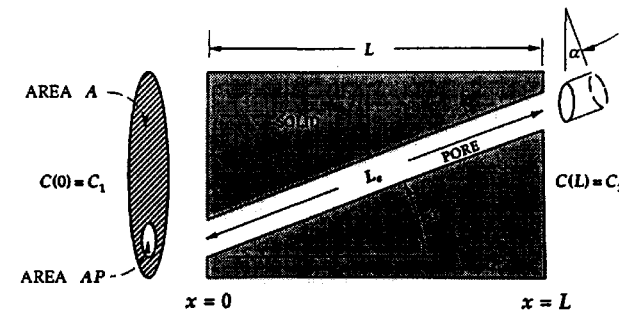


Figure 9.1 Idealized cylindrical pore within a solid matrix through which diffusion occurs.

The complicated geometry of a soil relative to diffusion path length and cross sectional area is usually described in terms of two parameters - tortuosity and porosity. We assume here that isothermal conditions prevail, the bulk volume of the soil remains constant, the soil solids are inert and for convenience, we consider gaseous diffusion in one dimension within a completely dry soil schematically shown in Fig. 9.1. For steady state conditions with  $C(0) = C_1$  and  $C(L) = C_2$ , the diffusion flux for the cylindrical pore of length  $L_c$  from (9.1) becomes

$$q = -D_o A_c \left( \frac{C_2 - C_1}{L_c} \right) \quad (9.2)$$

where  $D_o$  is the gaseous diffusion coefficient,  $A_c = APL/L_c$  the cross sectional area of the cylindrical pore,  $P$  the porosity and  $A$  the cross sectional area of the bulk soil. Similarly, for the bulk soil of length  $L$  (9.1) becomes

$$q = -DA \left( \frac{C_2 - C_1}{L} \right) \quad (9.3)$$

Equating (9.2) and (9.3) we have

$$D = D_o P (L/L_c)^2 \quad (9.4)$$

which is of a form suggested by Buckingham (1904) where  $(L/L_c)^2$  is the called tortuosity and equals  $\cos^2 \alpha$ . Penman's (1940) commonly used value of  $(L/L_c)^2 = 0.66$  yields an angle of  $0.61$  or  $35^\circ$  between the pore and the solid particle of soil. Marshall (1958) and Millington and Quirk (1959) empirically raised the power of  $P$  to  $3/2$  and  $4/3$ , respectively, and deleted  $(L/L_c)^2$  in (9.4) to account for the tortuosity of the average diffusion path.

Equations similar to (9.4) are easily derived for diffusion coefficients in partially water saturated soil as well as for solute diffusion in saturated and unsaturated soils. For example, Sallam et al. (1984) experimentally showed that the product  $P(L/L_c)^2$  in (9.4) for gaseous diffusion in unsaturated soils is more nearly equal to  $a^{3.10} P^{-2}$  rather than  $a^{10/3} P^{-2}$  (Millington and Quirk, 1959) where  $a$  is the air-filled porosity. Even for isothermal conditions, in addition to the concentration gradient, we have oversimplified our discussion here by neglecting pressure gradients and external forces acting unequally on the various gaseous and solute species. And, we should remember that the value of a diffusion coefficient depends upon the nature of the counter-diffusing gaseous or solute species.

### 9.1.2 Electrostatic and Electrokinetic Forces

Electric force fields always exist within the pore structure of soils owing to the electric charge possessed by the walls of soil pores. The charge per unit pore wall area is caused by isomorphous substitution of atoms in the tetrahedral and octahedral layers of the clay minerals as well as the presence of the Si-O-H (silanol) group on quartz, kaolin minerals and other surfaces like organic matter (-OH and -COOH). The magnitude of the former is fixed while that of the latter depends upon pH and concentration of the soil solution. In general, small highly charged ions cause the viscosity of the soil solution to increase while

large monovalent ions cause the viscosity to decrease. The electrostatic fields of the ions cause polarization and a binding of surrounding water molecules which alter the kinetic properties of soil water. The hydrophilic nature of most soil particles is attributed to the attraction of hydrated cations by the electrostatic field of soil particles and to the hydrogen bonding of water to the clays (Low, 1961). The mobility of both water and ions in the region of the pore walls is reduced below that in bulk solutions (Kemper, 1960; and Dutt and Low, 1962). The impact of the electric field on ions and water is more pronounced in clayey soils and depends upon the ionic concentration and distance from the pore wall.

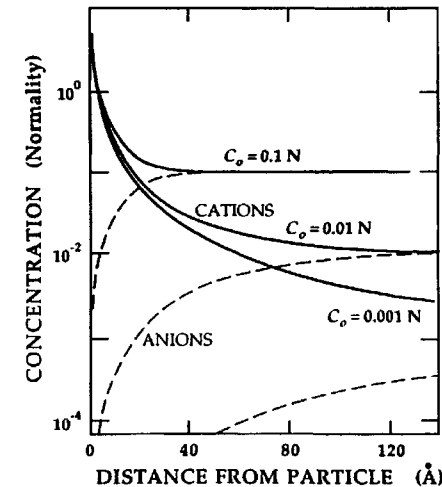


Figure 9.2. Distributions of cations and anions in the vicinity of a clay particle surface for three different solution concentrations.

Gouy (1910) described the distribution of cations as a function of distance from a negatively charged flat surface by equating the electrostatic force causing cations to move toward the surface to that from their thermal motion causing them to diffuse away from the surface. We see in Fig. 9.2 that the extent of the unequal distribution of cations and anions away from the surface depends inversely upon the total concentration  $C_o$  of the solution. And, we note from Fig 9.3 for cylindrical pores with a wall having a net negative charge and filled with a solution of concentration  $C_o$  that the concentration distribution across the pores depends upon the magnitude of the pore radius. In the center of large pores the concentrations of cations and anions are identical while in the center of small pores owing to the electric field, the cationic concentration exceeds that of anions.

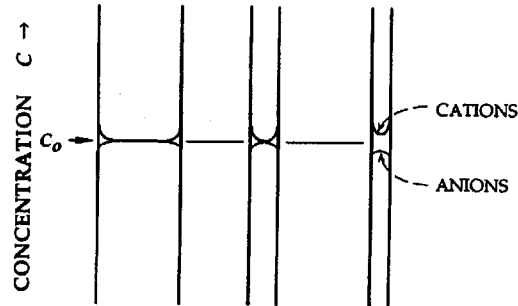


Figure 9.3. Distributions of cations and anions within capillary tubes having three different radii.

When redistribution of soil water occurs by air entering larger water-filled pores, solutes within water films remaining in the "emptied" large pores diffuse and mix with those in water-filled smaller pores achieving a new equilibrium which manifests different concentration distributions in all pores - large and small. Recognizing that the rates of water and solute redistribution are interdependent, equilibrium distributions of solute and water (hysteresis) both depend upon the rate at which hydraulic equilibrium is reached (Davidson et al., 1966).

As water moves through pores, cations and anions unequally distributed across the pores because of the negatively charged pore walls are swept along with the water. Consequently, a differential charge builds up along the length of flow which tends to retard water flow. This differential charge is called streaming potential. Similarly, if an electrical potential difference is established across a soil, ions moving within the electric field will create a water flux. Analytical descriptions of streaming potential, electroosmosis, electrophoresis and sedimentation potential are found in the literature (e.g. Nerpin and Tchudnovskii, 1967, and Taylor and Ashcroft, 1972). Each process contributes to the behavior of solutes and water at the pore scale and offers an opportunity for understanding and managing solute movement and retention in soil profiles.

### 9.1.3 Other Reactions

Constituents in the gas, liquid and solid phases of soil continually reacting with each other through a variety of chemical and biological pathways contribute to the presence and behavior of particular solutes in soil profiles. Applicable equilibrium and nonequilibrium chemical concepts such as oxidation-reduction, solubility-precipitation, association-dissociation, acid-base and exchange-adsorption are described by Freeze and Cherry (1979) and Luckner and

Schestakow (1991). Descriptions of microbiological reactions and pathways are available (e.g. Bazin et al., 1976) as well as those involving root systems of higher plants (e.g. Nye and Tinker, 1977). A full understanding of solute transport requires a knowledge of the information contained in these and other references.

## 9.2 MISCIBLE DISPLACEMENT IN A CAPILLARY

The oldest approach to analytic descriptions of miscible displacement in soils and other porous media is that of the displacement of a fluid by a second miscible fluid within a capillary tube. Consideration was focused upon the average displacement velocity and geometric boundaries with little concern for chemical or microbial processes.

### 9.2.1 Displacement without Molecular Diffusion

From the definition of viscosity, the force per unit area  $\tau$  required to shear a fluid of viscosity  $\eta$  is

$$\tau = -\eta \frac{dv}{dr} \quad (9.5)$$

where  $v$  is the velocity of the fluid and  $r$  the coordinate normal to the force. The velocity distribution within a horizontal capillary tube of radius  $a$  during steady, uniform flow caused by a pressure difference  $\Delta p$  across its length  $L$  is the result of an equilibrium between the pressure and shearing forces acting on the fluid. Hence, for the capillary tube

$$\pi r^2 \Delta p + 2\pi r L \eta \frac{dv}{dr} = 0 \quad (9.6)$$

Integrating (9.6) between the limits  $r = r$  and  $r = a$  (where  $v = 0$ ), we have the well known parabolic velocity distribution

$$v(r) = 2v_0 \left(1 - \frac{r^2}{a^2}\right) \quad (9.7)$$

where  $v(0) = 2v_0$ . The volumetric flow rate  $Q$  ( $\text{cm}^3 \cdot \text{s}^{-1}$ ) through the capillary is easily obtained by integrating  $v(r)$  with the areal cross-section of the capillary

$$Q = \int_0^a 2\pi r v(r) dr = 4\pi v_0 \int_0^a \left(r - \frac{r^3}{a^2}\right) dr \quad (9.8)$$

or

$$Q = a^2 \pi v_0 = \frac{a^4 \pi \Delta P}{8\eta L} \quad (9.9)$$

And the average velocity  $\bar{v}$  of fluid flowing within a capillary tube is simply

$$\bar{v} = \frac{1}{\pi a^2} \int_0^a 2\pi r v(r) dr = \frac{4v_0}{a^2} \int_0^a \left(r - \frac{r^3}{a^2}\right) dr \quad (9.10)$$

which leads to  $\bar{v} = v_0$ .

If we assume no molecular diffusion and rely solely on (9.7) to describe the fluid velocity, what will be the distribution of a second fluid of concentration  $C_o$  as it displaces a fluid of zero concentration initially within a capillary? Consider the solution  $C_o$  enters the tube at  $x = 0$  at time  $t = 0$ . The concentration  $C$  averaged over the cross section of the capillary at distance  $x$  is

$$C_a = \frac{1}{\pi a^2} \int_0^a 2\pi r C(r) dr$$

or as a function of distance and time is

$$C_a(x, t) = C_o(1 - x/2v_o t). \tag{9.11}$$

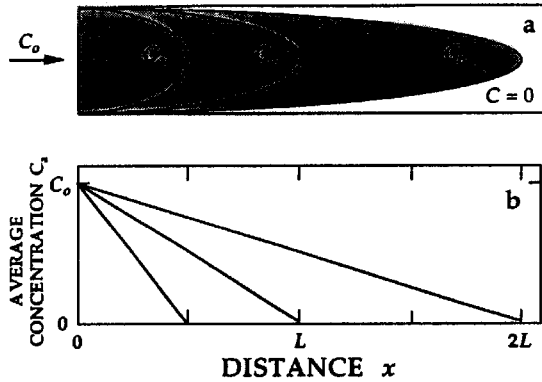


Figure 9.4. Parabolic velocity distributions of an invading solution  $C_o$  within a capillary (upper) give rise to linear average concentration distributions along the tube (lower).

In Fig. 9.4, the paraboloid of the displacing fluid  $C_o$  within the capillary gives rise to a linear concentration distribution. When the invading front of  $C_o$  has reached a distance  $2L$ , the average concentration across the plane normal to the capillary at a distance of  $L$  is  $C_o/2$ . Interestingly, the average concentration of the fluid moving across the plane  $L$  at that instant is not  $C_o/2$  but  $3C_o/4$ . The average concentration of fluid moving past  $x = L$  (see Fig. 9.5a) is

$$C_a = \frac{\text{mass of solute moving past } x=L}{\text{volume of fluid moving past } x=L}$$

$$C_a = \frac{C_o \int_0^{r'} [2v_o(1-r^2/a^2)] 2\pi r dr}{\int_0^a [2v_o(1-r^2/a^2)] 2\pi r dr} \tag{9.12}$$

where  $r' = a(1 - L/2v_o t)^{1/2}$ , the radial boundary between the displacing fluid ( $C = C_o$  for  $r < r'$ ) and the original fluid ( $C = 0$  for  $r > r'$ ). Integrating (9.12) leads to

$$\begin{aligned} C_a(t)/C_o = 0 & & v_o t / L \leq 0.5 \\ & = 1 - L^2 / 4v_o^2 t^2 & v_o t / L > 0.5 \end{aligned} \tag{9.13}$$

or

$$\begin{aligned} C(p)/C_o = 0 & & p \leq 0.5 \\ & = 1 - 1/4p^2 & p > 0.5 \end{aligned} \tag{9.14}$$

where  $p = v_o t / L$  and is the ratio of the volume of fluid passing  $x = L$  to the volume of the capillary between  $0 \leq x \leq L$ . Pore volume of effluent or simply pore volume is the name commonly used for  $p$ . The value of  $C = 3C_o/4$  for  $p = 1$  and approaches unity as  $p \rightarrow \infty$ , see Fig. 9.5b. Even for such a simple geometry as a capillary tube, the concentration distribution within the tube (Fig. 9.4b) is not easily reconciled with the shape of the concentration elution curve (Fig. 9.5b).

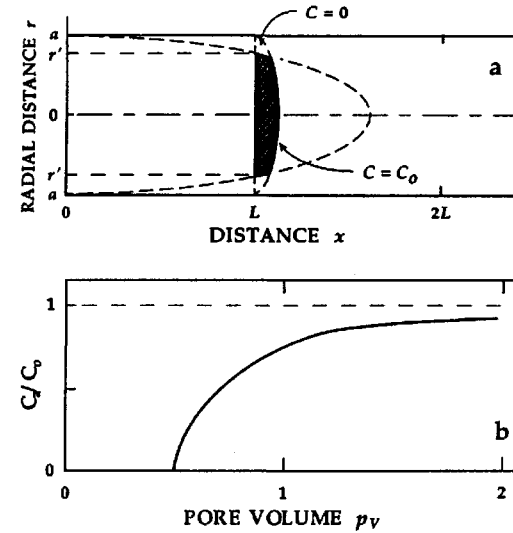


Figure 9.5. a. Cross sectional diagram of an elementary volume of fluid moving within a capillary. b. Average relative concentration of fluid leaving a capillary of length  $L$  as a function of pore volume of effluent.



### 9.3 MISCIBLE DISPLACEMENT IN SURROGATE POROUS MEDIA

The mixing and interactive processes described in section 9.1 for simple, well-defined geometries and materials provide a basis for understanding transport in soils. Unfortunately, the rigor of solutions exemplified by those of Taylor (1953) gives way to that of empirical or statistical formulations owing to our inability to mathematically define the geometry of the soil pore system or to measure parameters descriptive of the displacement processes that can be translated from the pore scale through intermediate scales (including that of a REV) to that of a pedon or field. Miscible flow in a porous medium differs from that in a single capillary owing to meandering paths of water and solutes within and between irregularly shaped pores. The spreading or dispersion of the solute caused by convective transport with the water can be qualitatively visualized in Fig. 9.6a for a simplified soil, or in Fig. 9.6b for an idealized 2-dimensional network of square soil particles. In both figures, the invading stream of solute partitions itself according to the microscopic pore water velocities occurring between the soil particles. At still a smaller scale, the water velocity is zero at the particle surface, departs markedly from the mean flow direction and approaches a zero value in the vicinity of dead-end pores (Fig. 9.7). These pathways and pore water velocities, severely altered with slight changes of water content, have yet to be quantitatively evaluated. In the near future, computer-aided micro tomography and nuclear magnetic resonance techniques will provide an opportunity to ascertain the exact nature of the velocities at the pore scale. Without such observations, our understanding of certain facets of miscible displacement in soils has been enhanced by considering surrogate porous media having simplified or empirical pore geometries. These equations developed to describe the displacement of fluids in such media are usually deficient of physical and mathematical rigor at the pore scale and often contain empirical coefficients not easily related to natural soils.



Figure 9.7. Examples of microscopic pathways and dead-end pores.

#### 9.3.1 Displacement in Capillary Networks

Descriptions of idealized soil pores having capillary shapes include some mechanism for transport between parallel capillaries or allow one or more capillary tubes of differing radii to be joined at their ends at common junctions (e. g. Marle and Defrenne, 1960). The concept of random networks of capillary tubes provides insights to the meandering paths of displacing fluids.

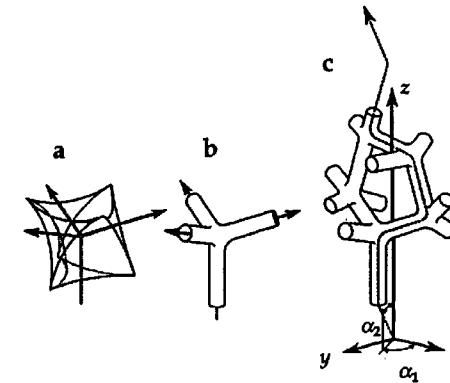


Figure 9.8. Diagram of pore space. a. Tetrahedral pore between four spheres, b. pore schematized by a canal bifurcation and c. random path chosen by a solute particle through the canal system.

The capillary tube network (de Josselin de Jong, 1958) illustrated in Fig. 9.8 stems from the tetrahedral pore between four closely packed spheres being represented by a junction of four capillaries. The randomness of the capillaries originates from the assumption that their positions are dictated by a random arrangement of soil particles. With  $z$  being the direction of principal flow, the direction of each segment of the capillary network is described by the angles  $\alpha_1$  and  $\alpha_2$ . de Josselin de Jong neglected molecular diffusion and assumed that the velocity of a fluid particle was that of the mean velocity across the capillary diameter. Assuming that every capillary segment is of length  $l$  and the fluid velocity within each segment is proportional to  $\cos \alpha_2$ , the residence time  $t_i$  for a fluid particle in segment  $i$  is  $t_i = t_R / \cos \alpha_2$  where  $t_R$  is the minimum residence time of a fluid particle traveling in a segment oriented in the direction of principal flow. Hence, a fluid particle traveling in a segment oriented in the direction  $(\alpha_1, \alpha_2)$  for a time  $\Delta t$  with a velocity  $(l/t_R)\cos \alpha_2$  will deviate from the mean flow path by

$$\Delta z = \frac{l \Delta t \cos^2 \alpha_2}{t_R} \quad (9.22)$$

and

$$\Delta r = \frac{l \Delta t \sin \alpha_2 \cos \alpha_2}{t_R} \quad (9.23)$$

These deviations lie on a sphere centered at  $l \Delta t / 2t_R$  having a radius  $l \Delta t / 2t_R$ .

The dispersion of many fluid particles having passed through a large number of capillary segments resembles that of Brownian movement, but translated in the direction of the principal flow. Hence, the maximum concentration of an injected solute travels at the mean velocity of the fluid  $l/(3t_R)$ . With this simple capillary network composed of segments of invariant length, de Josselin de Jong was the first to show that the transverse apparent diffusion coefficient is smaller than the longitudinal apparent diffusion coefficient. He also showed that the magnitude of the longitudinal apparent diffusion coefficient depends upon the distance traveled. Subsequently, Saffman (1959, 1960) derived a similar, but more general model where the path of the fluid particle was regarded as a random walk with the direction, length and duration of each step being random variables. He accounted for pure molecular diffusion and the interaction between molecular diffusion and fluid convection.

### 9.3.2 Miscible Displacement as a Random Walk Process

Statistical concepts have been applied to solute and water transport through porous media at the pore scale primarily because of the difficulty of integrating differential equations of motion with poorly or undefined complex boundary conditions. Danckwerts (1953), Scheidegger (1954) and others have assumed that a simple random walk stochastic process can be used to describe transport in a fluid-saturated homogeneous, isotropic porous medium generally considered chemically inert. Here the exact nature of the path followed by fluid particles theoretically obeying Navier-Stokes equation in the porous system is not known. The velocity or position of a water or solute particle is the random variable and as the particle passes through the porous system, it eventually encounters all situations that are possible at any one given time. The probability distribution function  $w$  for any water particle at various points along the random path (Scheidegger, 1954) is given by

$$w(x, y, z, t) = \frac{1}{(4\pi Dt)^{3/2}} \exp \left[ -\frac{(x-v_x t)^2 + (y-v_y t)^2 + (z-v_z t)^2}{4Dt} \right] \quad (9.24)$$

where  $v_x$ ,  $v_y$  and  $v_z$  are the Darcy velocity components [components of  $q$  in (5.32) each divided by  $\theta$ ] in directions  $x$ ,  $y$  and  $z$ , and  $D = \sigma^2/2t$  where  $\sigma^2$  is the variance of  $w(x, y, z, t)$ . Day (1956) described in detail the connection between  $w(x, y, z, t)$  and the macroscopic concentration of a solute being displaced in a saturated sand.

Recognizing that (9.24) is proportional to the solute concentration and knowing that (9.24) satisfies classical diffusion equations, Danckwerts (1953)

used solutions of

$$\frac{\partial C}{\partial t} = D \frac{\partial^2 C}{\partial X^2} \quad (9.25)$$

subject to appropriate initial and boundary conditions to describe the displacement of solutes through fluid-saturated porous media where  $X = (x - v_x t)$ . He noted that the value of  $D$  must be determined empirically and would presumably depend upon the viscosity, density and velocity of the fluid, and on the size and shape of the solid particles. He called  $D$  the "diffusivity" while Scheidegger named it the "factor of dispersion".

### 9.3.3 Displacement in a Representative Elementary Volume

The random capillary models described above were made somewhat more physically realistic [Bear and Bachmat, 1967] by deriving the idea of a representative elementary volume at the macroscopic scale from microscopic quantities at the pore scale averaged over many pores. Molecular diffusion and convection of solutes and water flowing within individual pores are described at the pore scale while the spreading or dispersion of solutes with water as it curves around and between soil particles through sequences of pores occurs at the macroscopic scale.

Bear and Bachmat envisioned the porous medium as a network of randomly interconnected narrow channels of varying length, cross section and orientation. The chemically inert, non compressible liquid of variable viscosity and density saturating the pores obeys Poiseuille's law and has two components - a solvent and a solute. No surface phenomena between the solid particles and the liquid take place. After deriving and averaging mass conservation and movement equations for the liquid in and across a channel, these local equations were averaged in a REV to obtain macroscopic equations. Details of all assumptions and the various averaging processes that lead to macroscopic equations containing average non random variables and parameters assigned to the centroid of the REV are given by Bear (1969). We repeat here their final equation of mass conservation in one direction avoiding the second-rank tensorial notation necessary for a three dimensional analysis

$$\frac{\partial C}{\partial t} = \frac{\partial}{\partial x} \left[ (D_c + D_m) \frac{\partial C}{\partial x} \right] - \frac{\partial(vC)}{\partial x} \quad (9.26)$$

where  $v$  and  $C$  are average values within the REV and  $D_c$  and  $D_m$  are the coefficient of convective (or mechanical) dispersion [ $L T^{-2}$ ] and coefficient of molecular diffusion [ $L T^{-2}$ ], respectively. Combining the latter coefficients into a single term  $D_s$  (commonly called the hydrodynamic dispersion coefficient or the apparent diffusion coefficient), we have

$$\frac{\partial C}{\partial t} = \frac{\partial}{\partial x} \left[ D_s \frac{\partial C}{\partial x} \right] - \frac{\partial(vC)}{\partial x} \quad (9.27)$$

for which many investigators have sought theoretical or experimental

relationships between the value of  $D_a$  (which embraces solute mixing at both the pore scale and the pore-sequence scale within an REV) and the value of  $v$  (the average pore water velocity usually estimated by the ratio of the Darcian flux density and water content  $\theta$ ).

The results of several studies summarized by Pfannkuch (1962) related the value of  $D_a$  to the Peclet number of molecular diffusion  $Pe$  equal to  $vd/D_m$  where  $d$  is the mean solid particle size or other characteristic length of the porous medium. Recognizing that the effects of both molecular diffusion and convection on solute mixing in typical one-dimensional experiments were difficult separate, Fried and Combarous (1971) suggested five ranges of Peclet numbers or zones to delineate the relative magnitudes of each process. For laboratory or field soils, we suggest that the following four zones will generally suffice except under some field conditions when turbulent flow down large fissures and cracks prevails during periods of rapid infiltration:

Zone 1	$Pe < 0.3$	$D_a = D_m$	$D_c \ll D_m$
Zone 2	$0.3 < Pe < 5$	$D_a = (D_m + D_c)$	$D_c \approx D_m$
Zone 3	$5 < Pe < 20$	$D_c < D_a < (D_c + D_m)$	$D_c > D_m$
Zone 4	$Pe > 20$	$D_a = D_c$	$D_c \gg D_m$

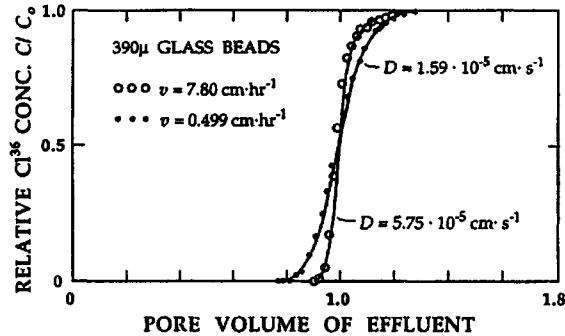


Figure 9.9. Breakthrough curves of  $^{36}\text{Cl}$  for the displacement of 0.10 N NaCl at two flow rates through a uniform column of glass beads.

Zones 1 and 2 are illustrated in Fig. 9.9 for a miscible displacement experiment conducted with a column uniformly packed with 390 $\mu$  glass beads initially saturated with 0.10 N NaCl. This initial solution was displaced at two different pore water velocities (0.499 and 7.80  $\text{cm}\cdot\text{h}^{-1}$ ) with a chemically identical solution containing  $\text{Na}^{36}\text{Cl}$  to observe the mixing process and to match the concentration distribution measured at  $x = 30$  cm with the solution of (9.27) subject to conditions

$$\begin{aligned} C &= 0 & x > 0 & t = 0 \\ C &= C_0 & x = 0 & t > 0 \\ C &= 0 & x \rightarrow \infty & t \geq 0 \end{aligned} \quad (9.28)$$

where  $C_0$  is the concentration of  $^{36}\text{Cl}$ . For each of the two pore water velocities, Fig. 9.9 shows measured values of the relative concentration  $C/C_0$  and smooth curves satisfying (9.27) and (9.28) fitted to the data through the selection of the only unmeasured entity  $D_a$  in

$$\frac{C(x,t)}{C_0} = \text{erfc}\left(\frac{x-vt}{\sqrt{4D_a t}}\right) + \exp\left(\frac{vx}{D_a}\right) \text{erfc}\left(\frac{x+vt}{\sqrt{4D_a t}}\right) \quad (9.29)$$

where  $\text{erfc}$  the complementary error function has been defined earlier by (9.18). Values of  $D_a$  for each value of  $v$  satisfy the equation (Fried and Combarous, 1971)

$$\frac{D_a}{D_m} = 0.67 + \alpha \left(\frac{vd}{D_m}\right)^n \quad (9.30)$$

where  $D_m = 1.98 \cdot 10^{-5} \text{ cm}^2\cdot\text{s}^{-1}$  (Wang, 1952) and  $d = 3.9 \cdot 10^{-2}$  cm. Experimentally determined values of  $\alpha = 0.51$  and  $n = 1.02$  agree with those suggested by Fried and Combarous (1971). For the slower pore water velocity (0.499  $\text{cm}\cdot\text{h}^{-1}$ ) with  $Pe = 0.27$  (corresponding to the upper end of Zone 1), 83% of the mixing is caused by molecular diffusion. For the faster velocity (7.80  $\text{cm}\cdot\text{h}^{-1}$ ) with  $Pe = 0.43$  (corresponding to the lower end of Zone 2), only 23 % of the mixing is caused by molecular diffusion.

Equation (9.30) is frequently reduced to

$$D_a = 0.67 D_m + \beta v^n \quad (9.31)$$

for Zones 3 and 4 with the molecular diffusion term neglected and the value of  $n$  taken as unity. In such instances,  $\beta$  is called the dispersivity.

Various investigators have used (9.27) or many similar diffusion type equations such as (9.25) with particular assumptions regarding the role of longitudinal and transverse molecular diffusion to theoretically or experimentally relate  $D_a$  to some function of  $v$  such as (9.30) or (9.31). Twenty five years ago Simpson (1969), writing a review article on the relationship between pore water velocity and the value of the longitudinal dispersion coefficient, stated, "The critical experiments remain to be performed: a systematic investigation of the effect on dispersion of changes in the molecular diffusivity". Somewhat later Sposito et al. (1979) presented a critical review of different theories used to describe solute transport through porous media. His remarks relative to theories based upon fluid mechanics and kinematic approaches employing various statistical techniques reveal major opportunities to improve our understanding of miscible displacement in surrogate porous materials. Earlier reviews by Fried and Combarous (1971) and Bear (1969) also provide additional insights for future research.

#### 9.4 ONE-DIMENSIONAL LABORATORY OBSERVATIONS

The displacement of one fluid by another miscible fluid in a soil studied either in the laboratory or the field offers theoretical and experimental challenges that have only partially been explored despite 30 years of recent investigation. For water infiltrating into a deep, homogeneous, water-saturated soil, we see in Fig. 9.10 that a solute of concentration  $C_o$  maintained at a point on the soil surface is dispersed vertically and horizontally. The velocity of the soil solution varies in both magnitude and direction owing to the distribution of irregularly shaped pores within the soil. Along transect A-A', the initial concentration  $C_o$  at  $z = 0$  gradually diminishes to zero. Similarly, the concentration distribution normal to the average flow along transect B-B' gradually broadens with soil depth.

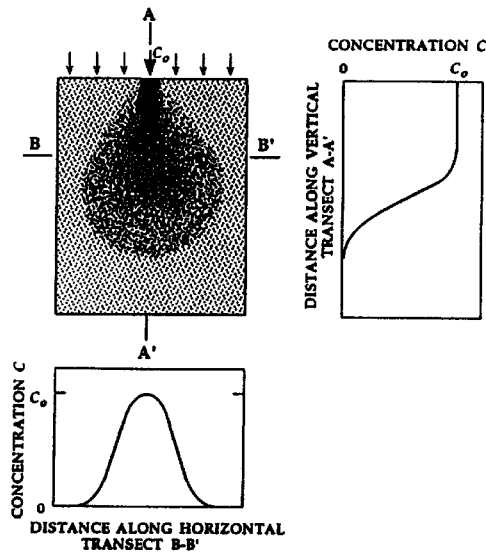


Figure 9.10. A solution of concentration  $C_o$  being introduced at one point on the surface of a uniform, water-saturated soil during steady state infiltration. Right: Concentration distribution along vertical transect A-A'. Bottom: Concentration distribution along horizontal transect B-B'.

One dimensional soil columns studied in the laboratory provide a simple means of quantifying the mixing, spreading or attenuation of the solute schematically presented in Fig. 9.10. An apparatus is required to maintain steady state flow and invariant soil water content conditions when the initial soil

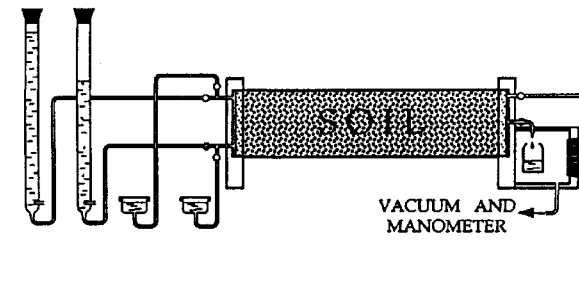


Figure 9.11. Laboratory apparatus for conducting miscible displacement experiments.

solution is invaded and eventually displaced by a second miscible solution. No mixing of the two solutions should occur at their boundary before entering the soil column, and samples of effluent to be analyzed for solute concentration has to be collected without disturbing the steady state flow conditions. A cross sectional sketch of a typical apparatus is given in Fig. 9.11. Details of its construction and operation are available (e. g. Nielsen and Biggar, 1961).

##### 9.4.1 Breakthrough Curves

Without first considering specific physical, chemical or biological mechanisms involved in miscible displacement, much can be learned from a general description of continuous flow systems (Danckwerts, 1953). Let the volume of the soil column occupied by soil solution be  $V_o$  [ $L^3$ ] and the rate of inflow and outflow of the soil solution be  $Q$  [ $L^3 T^{-1}$ ]. If the initial soil solution identified by a solute concentration  $C_i$  is suddenly displaced by an incoming solution  $C_o$ , the fraction of this incoming solute in the effluent at time  $t$  [T] will be  $(C - C_i)/(C_o - C_i)$ , or for an initial concentration of zero, simply  $C/C_o$ . Plots of  $C/C_o$  versus pore volume of effluent ( $Qt/V_o$ ), commonly called breakthrough curves, describe the relative times taken for the incoming solution to flow through the soil column. Note that the definition of pore volume of effluent is not restricted to water-saturated conditions but is applicable to all soil water contents. Any experimentally measured breakthrough curve may be considered one or a combination of any of the five curves shown in Fig. 9.12.

For Fig. 9.12a-c, the solute spreads only as a result of molecular diffusion and microscopic variations of the velocity of the soil solution, i. e. there is no interaction between the solute, water and soil particle surfaces. In these cases

$$\frac{Q}{V_o} \int_0^{\infty} (1 - C/C_o) dt = 1 \quad (9.32)$$

regardless of the shape of the curve. This equation expresses the fact that the original soil solution occupied exactly one pore volume or that the quantity of solute within the soil column that will eventually reach a chemical equilibrium with that in the influent and effluent is  $C_0 V_0$ . Note also that the area under the breakthrough curve up to one pore volume (area A in Fig. 9.12b and c) equals that above the curve for all values greater than one pore volume (area B), regardless of the shape of the curve. This latter statement is a direct result of (9.32), i. e.

$$\frac{Q}{V_0} \int_0^{V_0/Q} (C/C_0) dt = \frac{Q}{V_0} \int_{V_0/Q}^{\infty} (1 - C/C_0) dt. \quad (9.33)$$

Danckwerts (1953) defined holdback  $H_b$  as the left hand term of (9.33) having a range  $0 \leq H_b < 1$  for non reacting solutes. The concept of holdback is a useful qualitative description whenever interactions between solute, water and soil solids are minimal. It indicates the amount of the soil water or solutes not easily displaced. Values of  $H_b$  for unsaturated soils have been evaluated to be 3 to 4 times greater than those for saturated soils.

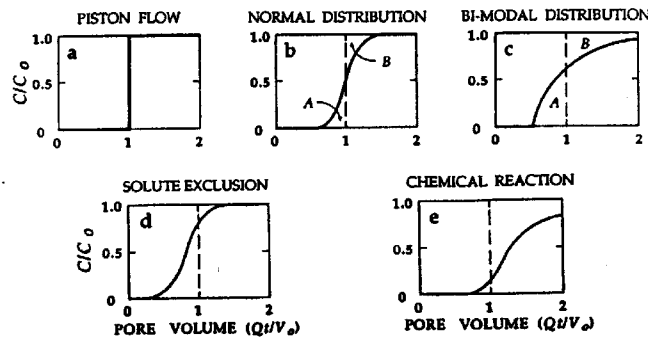


Figure 9.12. Types of breakthrough curves for miscible displacement.  $C/C_0$  is the relative concentration of the invading fluid measured in the effluent and pore volume is the ratio of the volume of effluent to the volume of fluid in the sample.

Piston flow (Fig. 9.12a) never occurs owing to solute mixing that takes place by molecular diffusion and variations in water velocity at the microscopic level within soil pores. A breakthrough curve obtained from a water-saturated Oakley sand (Fig. 9.13a) is characteristic of the longitudinal dispersion shown in Fig. 9.12b. Evidence for lack of solute-solid interaction is the fact that the areas described by (9.33) are nearly identical. A water-saturated soil composed of equal-sized aggregates manifesting a bimodal pore water velocity distribution yields the breakthrough curve given in Fig. 9.13b that illustrates the curve of Fig. 9.12c. With the areas of (9.33) for this curve being comparable, any interaction between the solute and the soil particles is negligible.

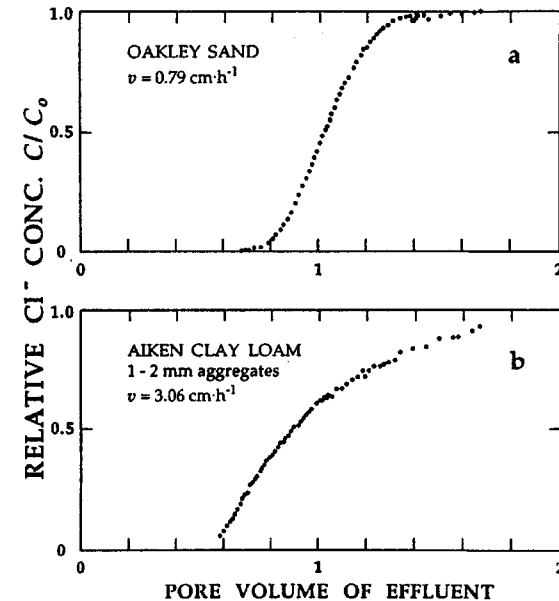


Figure 9.13. Chloride breakthrough curves for water-saturated a. Oakley sand and b. Aiken clay loam.

Figure 9.14 presents breakthrough curves for  $\text{Cl}^-$  and tritium (as tritiated water) from Columbia silt loam at two water contents and an average pore water velocity of approximately  $0.4 \text{ cm} \cdot \text{h}^{-1}$ . At a saturated water content of  $0.482 \text{ cm}^3 \cdot \text{cm}^{-3}$  (Fig. 9.14a), the  $\text{Cl}^-$  curve was measured to the left of one pore volume (given by the vertical broken line) and the tritium curve to the right of one pore volume. The translation of the  $\text{Cl}^-$  curve to the left of one pore volume is characteristic of the curve in Fig. 9.12d and results from the repulsion of the negatively charged  $\text{Cl}^-$  ions from the negatively charged soil particle surfaces. The translation of the tritium curve to the right of one pore volume is characteristic of the curve in Fig. 9.12e and results from adsorption and exchange of tritium in the soil. Despite these different interactions, the close proximity of the curves at  $C/C_0 = 0$  and their relative shapes near  $C/C_0 = 1$  indicate the more complete mixing of the tritium having the greater molecular diffusion coefficient. A solute having the greater diffusion coefficient mixes more completely with the water in stagnant and slowly conducting zones, thus delaying its appearance in the effluent. In this case, the initial breakthrough of the solute having the greater molecular diffusion coefficient is translated to the

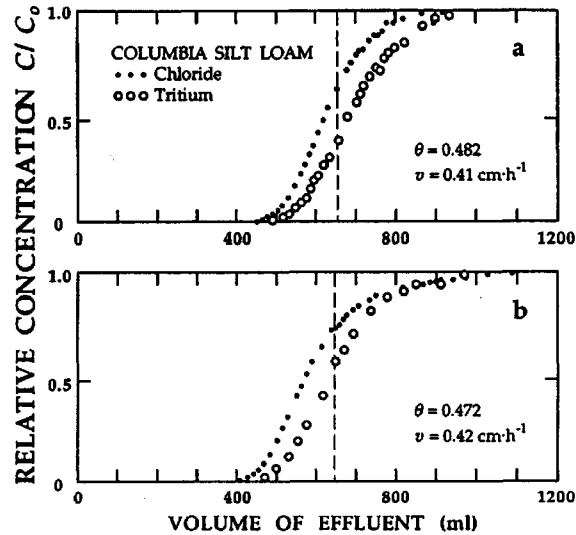


Figure 9.14. Chloride and tritium breakthrough curves for Columbia silt loam at soil water contents a.  $0.482 \text{ cm}^3 \cdot \text{cm}^{-3}$  and b.  $0.472 \text{ cm}^3 \cdot \text{cm}^{-3}$ . The vertical broken lines designate 1 pore volume.

right of that of the other solute. It should not be expected that the relative behavior of solutes described above would be the same for all velocities and different soils. For example, if one solute has a diffusion coefficient much greater than the other, it would be possible for it to not only invade the nearly stagnant zones but also diffuse downstream ahead of the other solute. In this case the faster diffusing solute will appear in the effluent earlier than the more slowly diffusing solute.

In Fig. 9.14b, decreasing the water content by only  $0.01 \text{ cm}^3 \cdot \text{cm}^{-3}$  translated both  $\text{Cl}^-$  and tritium curves to the left of one pore volume. Unsaturating the soil alters the pore water velocity distribution, allows some of the solute to arrive downstream earlier and increases the magnitude of holdback manifested by area A in Fig. 9.12. Desaturation eliminates larger flow channels and increases the volume of water within the soil which does not readily move. These almost stagnant water zones act as sinks to molecular diffusion. Later we shall discuss the opportunity afforded by controlling the water content and pore water velocity to change the leaching efficiency of field soils.

A more illustrative example of curves b, c and d in Fig. 9.12 are given in Fig. 9.15 from two columns of Oakley sand initially fully saturated with  $\text{Ca}^{2+}$

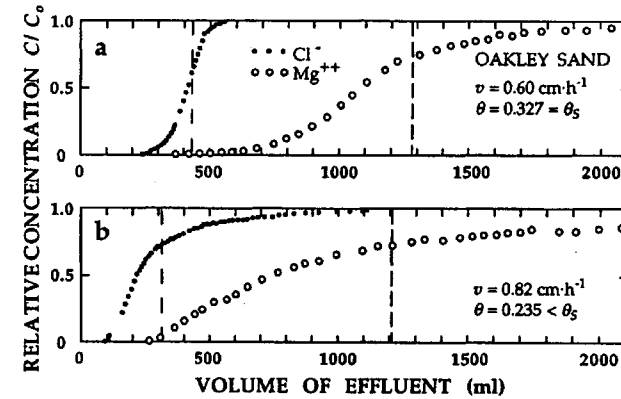


Figure 9.15. Chloride and magnesium breakthrough curves for initially  $\text{Ca}$ -saturated Oakley sand at soil water contents a.  $0.327 \text{ cm}^3 \cdot \text{cm}^{-3}$  and b.  $0.235 \text{ cm}^3 \cdot \text{cm}^{-3}$ . The two vertical, broken lines designate 1 pore volume for the chloride and the cation exchange capacity, respectively.

[cation exchange capacity of  $3.75 \text{ me} \cdot (100\text{g})^{-1}$ ] and  $0.1 \text{ N}$  calcium acetate flowing through them at a constant velocity while maintaining a constant water content. Breakthrough curves of  $\text{Cl}^-$  and  $\text{Mg}^{2+}$  for  $0.10 \text{ N}$   $\text{MgCl}_2$  displacing the calcium solution at water contents of  $0.327$  and  $0.235 \text{ cm}^3 \cdot \text{cm}^{-3}$  are presented in Fig. 9.15a and 9.15b, respectively. The positions of the  $\text{Cl}^-$  curves appear in the vicinity of the vertical lines representing the volume of solution in each soil column, while those of  $\text{Mg}^{2+}$  appear further to the right in the vicinity of another vertical line accounting for the cation exchange capacity. For the greater soil water content (Fig. 9.15a) the  $\text{Mg}^{2+}$  curve has the same characteristics as the  $\text{Cl}^-$  curve (similar to Fig. 9.12b) even though it is flatter and is displaced to the right (similar to Fig. 9.12d). Desaturating the soil water content (Fig. 9.15b) produces a  $\text{Cl}^-$  curve similar to Fig. 9.12c and a  $\text{Mg}^{2+}$  curve having the shape of Fig. 9.12c but a position illustrated in Fig. 9.12d. Depending upon the concentration and velocity of the displacing solution and the prevailing soil water content, the shapes and positions of breakthrough curves are governed by the characteristics of the cation exchange process as well as the mixing which occurs by the pore water velocity distribution, molecular or ionic diffusion and the spatial and temporal interaction of these processes.

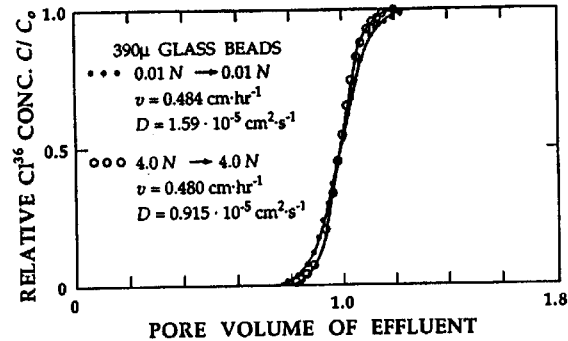


Figure 9.16. Breakthrough curves of  $^{36}\text{Cl}$  for 0.01 N NaCl displacing 0.01 N NaCl and for 4.0 N NaCl displacing 4.0 N NaCl in horizontal columns of water-saturated glass beads.

#### 9.4.2 Magnitude of the Diffusion Coefficient

The majority of inorganic cations, anions and solutes in soil solutions have diffusion coefficients in the order of  $10^{-5} \text{ cm}^2\cdot\text{s}^{-1}$  while organic cations, anions and solutes usually manifest much smaller values. These coefficients are moderately temperature dependent and slightly concentration dependent. The importance of their different magnitudes is apparent only at relatively small pore water velocities and often difficult to measure except under rigorously controlled laboratory conditions.

For a 30-cm long column of 390  $\mu$  glass beads, the results of two experiments observing the displacement of 0.01 N NaCl by an identical solution identified with a tracer of  $^{36}\text{Cl}^-$  and the displacement of 4.00 N NaCl by a similarly observed identical solution containing  $^{36}\text{Cl}^-$  are given in Fig. 9.16. With the pore water velocity for each experiment conducted at  $25 \pm 1^\circ\text{C}$  being about  $0.48 \text{ cm}\cdot\text{h}^{-1}$  (Zone 1 described in section 9.3.3) and the densities and viscosities of the displacing and displaced solutions being virtually identical, distinctly separate curves for each experiment are obtained owing primarily to the different self diffusion coefficients of  $^{36}\text{Cl}^-$  ( $1.98 \cdot 10^{-5}$  and  $1.24 \cdot 10^{-5} \text{ cm}^2\cdot\text{s}^{-1}$  for the concentrations of 0.01 and 4.00 N NaCl, respectively). At greater pore water velocities (Zones 2 through 4) where mixing by convection progressively dominates the displacement process, the importance of diffusion lessens. Accordingly, for most infiltration and redistribution events following rainfall or irrigation in field soils, a nominal value of the diffusion coefficient is assigned to either an inorganic or organic solute without discriminating between solute species or their concentrations. The impact of temperature on diffusional mixing remains obscure from investigation.

#### 9.4.3 The Impact of Density and Viscosity

The existence of concentration gradients of inorganic salts in the soil solution responsible for solute transfer by diffusion or as a result of convection guarantees that the displacing and displaced solutions do not generally have identical values of density or viscosity no matter how close their values. In soils, it is not uncommon to experience solutions of unequal density and viscosity. During the extraction of water from soil profiles by plants or by evaporation at the soil surface, the density and viscosity of the soil solution increase continually. Conversely the infiltration of rain or many irrigation waters causes the soil solution to be diluted. Fertilizers and other agrochemicals also alter these properties of the soil solution. The density and viscosity of the soil solution also differ from those of the bulk solution owing to the interaction of water and the soil particle surfaces especially in unsaturated soils or those soils having large clay contents (Dutt and Low, 1962).

When two superposed solutions of unequal density are accelerated in a direction perpendicular to their interface, the surface may be stable or unstable. Differences in density provide unbalanced forces while differences in viscosities account for unequal drag forces. For example, unstable flow occurs for particular velocities vertically downward when a dense, more viscous fluid displaces a less dense, less viscous fluid. Here, the unbalanced forces tend to accelerate the denser fluid into the less dense fluid below with the viscous drag of the lower fluid unable to counter-balance this acceleration. With this action "fingers" of the more viscous fluid invade those pore sequences occupied by the less dense fluid. For a 30 cm long vertical column of 390  $\mu$  glass beads, the breakthrough curve in Fig. 9.17 obtained for 0.01 N NaCl flowing upward at a velocity of 6.07

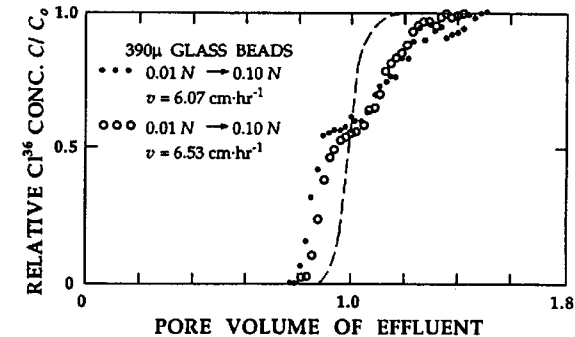


Figure 9.17. Breakthrough curves of  $^{36}\text{Cl}$  for 0.01 N NaCl displacing 0.10 N NaCl vertically upwards at two different flow velocities in columns of water-saturated glass beads. The broken line is a breakthrough curve for stable flow similar to that in Fig. 9.16.

cm·h<sup>-1</sup> and displacing the more dense and viscous 0.10 N NaCl exhibits unstable flow compared to that for stable flow (a curve from Fig. 9.16 shown as a broken line).

The stability of the displacement depends upon the viscosities and densities of the fluids, the permeability of the soil, and the direction and velocity of the displacement. If Darcy's equation is obeyed for steady movement with average pore water velocity  $v$  vertically upwards through a soil of permeability  $K_p$ , the interface between the two solutions will be unstable for

$$(\mu_2 - \mu_1)v + K_p(\rho_2 - \rho_1)g < 0 \quad (9.34)$$

where  $\rho$  is the density,  $\mu$  the viscosity and  $g$  the gravitational acceleration (Taylor, 1950). The subscripts 1 and 2 refer to the displaced and displacing fluids, respectively. Except for signs owing to the direction of the velocity, (9.34) also applies to movement vertically downward. Inequality (9.34) has been used extensively for immiscible fluids (e.g. Oatmans, 1962) and for miscible fluids (e.g. Wooding, 1959, and Brigham et al., 1961). For the immiscible fluids water displacing air during ordinary infiltration at the soil surface, the same principles apply for the potential development of fingers of water moving ahead of the average wetting front into the unsaturated soil profile. For miscible fluids, the thickness of the interface region is not constant and tends to increase owing to molecular diffusion. Hence, with the viscosity and density of the interfacial fluid being neither those of the displacing nor displaced fluid and with the pore geometry only implicitly considered through the value of  $K_p$ , (9.34) holds only approximately for soils.

#### 9.4.4 Influences of Solution Concentration and pH

Recalling from section 9.1.2, the surface charge characteristics of soil particles and colloids are of two general types - one having a constant surface charge and a variable surface potential, and the other having a constant surface potential and a variable surface charge (Bolt, 1979).

The interplay of these chemical effects on transport during the displacement of pulses of solution containing <sup>36</sup>Cl<sup>-</sup> through a water-saturated Oxisol (Nkedi-Kizza, 1979) is shown in Fig. 9.18. In Fig. 9.18a, as the concentration of the soil solution decreases from 0.1 to 0.001 N CaCl<sub>2</sub>, the <sup>36</sup>Cl<sup>-</sup> elution curves shift to the right with their maxima decreasing. At a pH of 4, Cl<sup>-</sup> is adsorbed. Owing to the fact that an equal number of negative and positive exchange sites exists at pH 3.6 for this soil, we expect <sup>36</sup>Cl<sup>-</sup> to be exchanged for their non radioactive isotopes on the clay surfaces. Differences in shapes and positions of the curves in Fig. 9.18a are a result of the concentration of the soil solution rather than caused by hydrodynamic and geometric aspects of the flow regime.

As the pH of the soil increases above 3.6, the relative proportion of negative to positive exchange sites increases. Thus, as shown in Fig. 9.18b for a constant soil solution concentration of 0.001 N, the <sup>36</sup>Cl<sup>-</sup> elution curve shifts to the left as the pH increases. At pH 9, the early arrival of <sup>36</sup>Cl<sup>-</sup> is indicative of a solute that is repelled from the predominantly negatively charged clay surfaces.

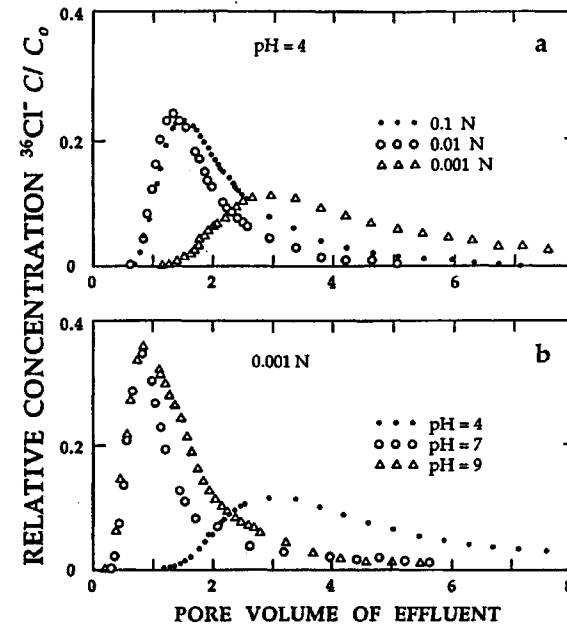


Figure 9.18. Breakthrough curves for a water-saturated, Ca-saturated Oxisol. a. <sup>36</sup>Cl<sup>-</sup> in a CaCl<sub>2</sub> solution displacing a solution of an identical chemical composition for three different concentrations at a pH of 4. b. <sup>36</sup>Cl<sup>-</sup> in a 0.001 N CaCl<sub>2</sub> displacing a solution of an identical chemical composition for three different values of pH.

Although arid soils usually are dominated by constant charge colloids and tropical soils by those of constant potential, all soils are mixtures of both, and hence their behavior under conditions that induce shifts in pH cannot be ignored.

#### 9.4.5 Influence of Displacement Length

The mixing and attenuation of a solute by convection depend upon the pore size distribution and the number of bifurcations experienced by the soil solution as water flows through its system of microscopic pores (recall Fig. 9.6). The greater the total macroscopic displacement length, the greater will be the

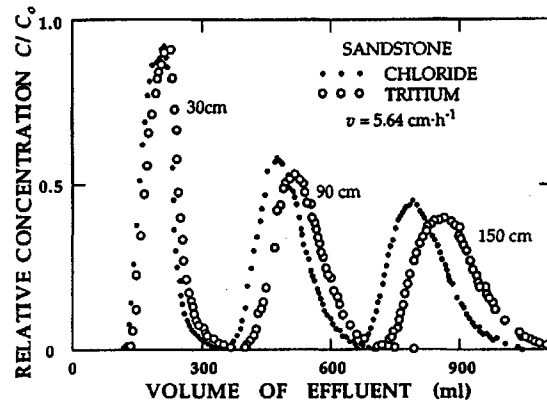


Figure 9.19. Chloride and tritium breakthrough curves for 30, 90 and 150 cm long, water-saturated sandstone columns.

opportunity for both convective and diffusive mixing. As the displacement length increases, both the number of bifurcations in the pore system and the time for molecular diffusion increase.

Corey et al. (1963) examined such a displacement as well as the nature of the pore structure of a uniform, consolidated sandstone by using five column lengths. Breakthrough curves for 75-ml pulses of tritiated  $\text{CaCl}_2$  solution (Fig. 9.19) displaced through three of the columns illustrate the progressive attenuation of the initial concentration  $C_0$  as the solute is displaced through greater macroscopic lengths. Having traveled 150 cm, the relative concentration was reduced to about 0.4. A practical implication of such attenuation is the dilution of a solute within a soil profile without leaching any of its total mass beyond a desired depth.

Note in Fig. 9.19 that the chloride appears earlier in the effluent than the tritium and the separation between the data increases with column length. This behavior demonstrates the differences of the interactions between each of the solutes and the sandstone matrix. By conducting displacement experiments with homogeneous columns of different lengths, the relative amounts of convective and molecular diffusive mixing can also be ascertained when a series of different average pore water velocities are employed. Corey et al. avoided the difficulty of packing long soil columns with sufficient uniformity by using a naturally occurring homogeneous sandstone.

## 9.5 THEORETICAL DESCRIPTIONS

With soil physicists continuing their propensity to focus on geometric considerations, soil chemists focusing on chemical reactions and ignoring geometric effects and soil microbiologists and plant nutritionists limiting their investigations to biotic absorption, our understanding of the leaching process in soil profiles remains incomplete. This deficiency reflects our present-day inability to integrate simultaneously the most relevant physical, chemical and biological processes in a unified theoretical framework. Only recently have there been attempts to model transport in multicomponent systems with consideration of microbial activity and chemical reactions (e.g. Yeh and Tripathi, 1991, Richter et al., 1992, and Šimůnek and Suarez, 1994). Several theoretical opportunities provide a basis for future experiments and analyses.

### 9.5.1 The Convective-Diffusion Equation

Here we derive the cornerstone of most theoretical descriptions of solute transport in porous media recognizing its form is tentative in several aspects besides being fraught with uncertainties of applicable temporal (Skopp, 1986) and spatial scales (Dagan, 1986) that are not easily resolved.

We begin with the prism element having edges of length  $\Delta x$ ,  $\Delta y$  and  $\Delta z$  given previously in Chapter 5 (Fig. 5.14). The difference between the mass of solute entering the prism and that leaving the prism equals the difference of the solute stored in the prism in time  $\Delta t$  providing that we account for any appearance (source) or disappearance (sink) of the solute within the prism by mechanisms other than transport. Hence, we obtain similar to (5.62) the equation of continuity of solutes  $S$  [ $\text{M L}^{-3}$ ]

$$\frac{\partial S}{\partial t} = - \left( \frac{\partial J_x}{\partial x} + \frac{\partial J_y}{\partial y} + \frac{\partial J_z}{\partial z} \right) + \sum_i \phi_i \quad (9.35)$$

where  $J_x$ ,  $J_y$  and  $J_z$  are the flux densities of solute in directions  $x$ ,  $y$  and  $z$  and  $\phi_i$  [ $\text{ML}^{-3}\text{T}^{-1}$ ] the  $i$ -th source or sink occurring within the prism usually considered irreversible during the time period over which the equation applies.

In general, soil solutes exist in both gaseous and aqueous phases as well as being associated with the solid organic and inorganic phases of the soil. Here, we neglect the fact that non aqueous polar and non polar liquids can also reside in soils and participate in the displacement process. We assume that at least some solutes in the soil solution are sufficiently volatile to consider their conient or transport in the gaseous phase. Hence, the total solute concentration  $S$  in (9.35) is

$$S = \rho_T C_S + \theta C + (P - \theta) C_G \quad (9.36)$$

where  $\rho_T$  is the soil bulk density [ $\text{M L}^{-3}$ ],  $C_S$  the solute adsorbed or exchanged on the soil solids [ $\text{M (M of dry soil)}^{-1}$ ],  $\theta$  the volumetric soil water content, and  $C$  the solute in solution [ $\text{M L}^{-3}$ ],  $P$  the porosity and  $C_G$  the solute in the soil air [ $\text{M L}^{-3}$ ].

The solute flux density  $J$  in (9.35) relative to the prism  $\Delta x \Delta y \Delta z$  is difficult to define unambiguously owing to the fact that the representative elementary volumes of each of the terms in  $J$  and  $S$  are not necessarily equal nor known, particularly for structured field soils. Each of the directional components of  $J$  is comprised of contributions of solute movement within the gaseous and liquid phases as well as along particle surfaces of the solid phase. We assume that solute movement along soil particle surfaces is nil or can be accounted for by functions relating the concentration of solutes in solution to that associated with the solid phase in (9.36). Hence, the solute flux density consists of three terms, one describing the bulk transport of the solute moving with the flowing soil solution, the second describing the solute moving by molecular diffusion and meandering convective paths within the soil solution and the third accounting for molecular diffusion in the gaseous phase. For the  $z$ -direction, we have

$$J_z = q_z C - \theta(D_c + D_m) \frac{\partial C}{\partial z} - (P - \theta) D_G \frac{\partial C_G}{\partial z} \quad (9.37)$$

where  $q_z$  is the Darcian flux,  $D_c$  and  $D_m$  are the coefficients of convective dispersion and molecular diffusion in the soil solution, respectively,  $D_G$  the molecular diffusion coefficient in the soil air and  $C_G$  the gaseous solute concentration in the soil air. Equations for  $J_x$  and  $J_y$  are identical to (9.37) when  $z$  has been replaced by  $x$  and  $y$ , respectively. We continue the analysis here for only the vertical soil profile direction  $z$  avoiding vectorial and tensorial notation.

Substituting (9.36) and (9.37) into (9.35), we obtain for a solute of the soil solution that does not volatilize into the soil air

$$\frac{\partial(\rho_T C_s)}{\partial t} + \frac{\partial(\theta C)}{\partial t} = \frac{\partial}{\partial z} \left[ \theta(D_c + D_m) \frac{\partial C}{\partial z} \right] - \frac{\partial(qC)}{\partial z} + \sum_i \phi_i \quad (9.38)$$

The first term of (9.38) describes the rate at which a solute reacts or exchanges with the soil solids. Its exact form (Helfferich, 1962) continues to be debated. We discuss both equilibrium and kinetic rate terms commonly used to describe this adsorption-exchange process in the next section.

With  $D_a = (D_c + D_m)$ , (9.38) reduces to

$$\frac{\partial(\rho_T C_s)}{\partial t} + \frac{\partial(\theta C)}{\partial t} = \frac{\partial}{\partial z} \left( \theta D_a \frac{\partial C}{\partial z} \right) - \frac{\partial(qC)}{\partial z} + \sum_i \phi_i \quad (9.39)$$

Although the source-sink term  $\phi_i$  in (9.38) or (9.39) has most often been considered in the absence of the rest of the equation in many disciplines, it is often approximated by zero- or first-order rate terms

$$\phi_i = \gamma\theta + \gamma_s \rho + \mu\theta C + \mu_s \rho_T C_s \quad (9.40)$$

where  $\gamma$  and  $\gamma_s$  are rate constants for zero-order decay or production in the soil solution and solid phases, respectively, and  $\mu$  and  $\mu_s$  are similar first-order rate constants for the two phases. For radioactive decay, physicists may safely assume that  $\mu$  and  $\mu_s$  are identical as well as assuming that both  $\gamma$  and  $\gamma_s$  are nil. Microbiologists, considering organic and inorganic transformations of soil solutes in relation to growth, maintenance and waste metabolism of soil microbes as a Michaelis-Menten process, often simplify their considerations to

that of  $\phi_i$  in (9.40). McLaren (1970) provided incentives to study such reactions as functions of both space and time in soil systems - a task not yet achieved by soil microbiologists, especially when the individual characteristics of each microbial species is quantified and not lumped together as a parameter of the entire microbial community. Agronomic or plant scientists consider  $\phi_i$  as an irreversible sink and source of solutes taking place in the vicinity of the rhizosphere of cultivated or uncultivated plants as a function of soil depth and time as well as some empirical function defining the root distribution.

For a solute that does not appreciably react with the soil particles, does not exist in the soil air and does not appear or disappear in sources or sinks, respectively, (9.39) reduces to

$$\frac{\partial C}{\partial t} = \frac{\partial}{\partial z} \left( D_a \frac{\partial C}{\partial z} \right) - \frac{\partial(vC)}{\partial z} \quad (9.41)$$

which is identical to (9.27) of Bachmat and Bear. For steady state flow in a homogeneous soil at constant water content, (9.41) reduces still further to

$$\frac{\partial C}{\partial t} = D_a \frac{\partial^2 C}{\partial z^2} - v \frac{\partial C}{\partial z} \quad (9.42)$$

which has been extensively used to develop empirical relations between the apparent diffusion coefficient  $D_a$  and the average pore water velocity  $v$ .

An intensively measured, field scale miscible displacement experiment conducted to ascertain the distributions of  $D_a$  and  $v$  was reported by Biggar and Nielsen (1976). During steady state water flow conditions, they measured the leaching of water soluble salts at six soil depths to 1.8 m within 20 subplots of a 150-ha field. For times  $0 < t \leq t_1$  the soil was leached steadily with water having a concentration  $C_o$  (chloride or nitrate). For times  $t < 0$  and  $t > t_1$  the soil was leached with water having a concentration  $C_i$ . In view of the large pore water velocities measured in their experiment, the appropriate initial and boundary conditions for the solution of (9.42) were

$$\begin{aligned} C &= C_i & z > 0 & & t = 0 \\ C &= C_o & z = 0 & & 0 < t \leq t_1 \\ C &= C_i & z = 0 & & t > t_1 \end{aligned} \quad (9.43)$$

The measured concentration  $C(z, t)$  was fitted to the solution of (9.42) subject to (9.43)

$$\begin{aligned} \frac{C - C_i}{C_o - C_i} &= \frac{1}{2} \left\{ \operatorname{erfc} \left[ \frac{z - vt}{(4D_a t)^{1/2}} \right] + \exp \left( \frac{vz}{D_a} \right) \operatorname{erfc} \left[ \frac{z + vt}{(4D_a t)^{1/2}} \right] \right\} - \\ &- \frac{1}{2} \left\{ \operatorname{erfc} \left[ \frac{z - v(t - t_1)}{[4D_a(t - t_1)]^{1/2}} \right] + \exp \left( \frac{vz}{D_a} \right) \operatorname{erfc} \left[ \frac{z + v(t - t_1)}{[4D_a(t - t_1)]^{1/2}} \right] \right\} \end{aligned} \quad (9.44)$$

at different locations within the field to obtain 359 values of  $(D_a, v)$  which are plotted against each other in Fig. 9.20. Values of  $D_a$  were logarithmically normally distributed with a mode of 4.0, a median of 85.1 and a mean of 367.6  $\text{cm}^2 \cdot \text{d}^{-1}$ . Values of  $v$  were also logarithmically normally distributed having a mode of 4.3, a median of 20.3 and a mean of 44.2  $\text{cm} \cdot \text{d}^{-1}$  (see Fig. 9.25). The solid

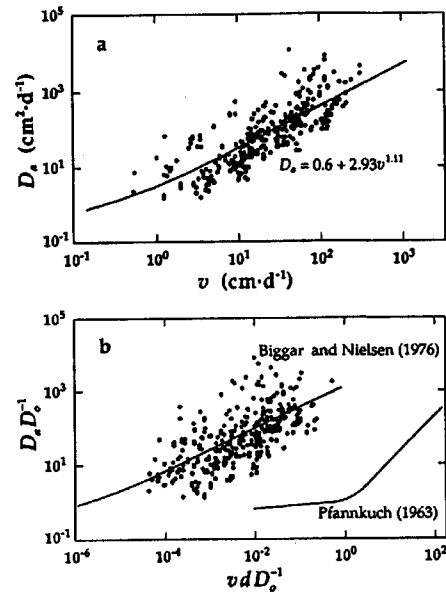


Figure 9.20. a. Field-measured values of the apparent diffusion coefficient  $D_a$  plotted against average pore water velocity  $v$ . b. Values of  $D_a D_o^{-1}$  plotted against Peclet number  $vdD_o^{-1}$  where  $D_o$  is the molecular diffusion coefficient and  $d$  is the mean soil particle diameter.

line in Fig. 9.20a obtained by regressing  $\ln(D_a - 0.6)$  versus  $\ln v$  is of the same form as (9.31). The value of 0.6 represents the molecular diffusion coefficient for the unsaturated soil taking into account the average tortuosity and the average soil water content during displacement. The same data plotted as  $D_a D_o^{-1}$  versus  $vdD_o^{-1}$  (Peclet number) in Fig. 9.20b where  $d$  is the mean soil particle diameter can be compared to those reported by Pfanckuch (1962) measured by several investigators in the laboratory using homogeneously packed columns. With the value of the coefficient  $\beta = 2.93$  being two orders of magnitude greater than found in the majority of laboratory column studies, the impact of soil structure and the large range of particle diameters and pore sizes on the dispersion of solutes in natural field soils is abundantly evident.

### 9.5.1.1 Solutes in Continual Equilibrium with the Solid Phase

Instantaneous adsorption or exchange reactions included in the first term of (9.38) are described by equilibrium isotherms  $C_s(C)$  of several different forms - mass action, linear, Freundlich, Langmuir or other functional forms (van Genuchten et al., 1974; Bolt, 1979; and Travis and Etnier, 1981).

The most common approach for modeling the first term of (9.38) has been to assume instantaneous adsorption or exchange as well as simple linearity between  $C_s$  and  $C$  [ $C_s = kC$  where  $k$  is the slope of the isotherm  $C_s(C)$  often referred to as the distribution coefficient  $K_d$ ]. If we put this linear isotherm in (9.39) we have

$$\frac{\partial(\rho_T k C)}{\partial t} + \frac{\partial(\theta C)}{\partial t} = \frac{\partial}{\partial z} \left( \theta D_a \frac{\partial C}{\partial z} \right) - \frac{\partial(qC)}{\partial z} + \sum_i \phi_i \quad (9.45)$$

which reduces to

$$R \frac{\partial C}{\partial t} = D_a \frac{\partial^2 C}{\partial z^2} - v \frac{\partial C}{\partial z} + \sum_i \phi_i \theta^{-1} \quad (9.46)$$

for steady state flow in a homogeneous soil and where  $R$  is a retardation factor ( $= 1 + \rho_T k \theta^{-1}$ ). Equation (9.46) has been solved for many conditions for both finite and semi-infinite systems (van Genuchten and Alves, 1982; Javandel et al., 1984). While the simplicity of a linear isotherm is a convenient feature for mathematically modeling, its limitations are clearly apparent owing to adsorption and exchange processes usually being nonlinear and depending upon the competing species in the soil solution (see Reardon, 1981; Miller and Benson, 1983; and Valocchi, 1984).

### 9.5.1.2 Solutes Not in Equilibrium with the Solid Phase

Diffusion-controlled or chemically controlled kinetic rate reactions included in the first term of (9.38) have been described in a variety of equations. We consider here three of the more popular formulations.

The most simplest formulation is that of a first order linear kinetic reaction where (9.39) is replaced by two coupled equations. Here, for steady state flow through a homogeneous soil without sources or sinks, we have

$$\begin{aligned} \frac{\rho_T}{\theta} \frac{\partial C_s}{\partial t} + \frac{\partial C}{\partial t} &= D_a \frac{\partial^2 C}{\partial z^2} - v \frac{\partial C}{\partial z} \\ \frac{\partial C_s}{\partial t} &= \alpha(kC - C_s) \end{aligned} \quad (9.47)$$

where  $\alpha$  is a first order rate constant. The success of this and similar rate models (e. g. Davidson and McDougal, 1973; van Genuchten et al., 1974) has been best when miscible displacement experiments have been carried out at relatively slow velocities when mixing is dominated by molecular diffusion. Nevertheless, under such conditions the values of  $\alpha$  and  $k$  may indeed be biased owing to the use of an average value of  $v$  which does not embrace the spatial distribution of the solute influencing the rate reaction within soil pores at the microscopic scale.

The second formulation gives more consideration to the microscopic pore water velocity by defining a bimodal distribution which partitions the soil water into mobile and immobile phases. In the mobile phase where soil water flows, solute behavior is described by a convective-diffusion equation. Inasmuch as water is stagnant in the immobile phase, solutes move in and out of this phase only by molecular diffusion. Zones of stagnant water derive from thin liquid films around soil particles, dead-end pores, non moving intra-aggregate water or isolated regions associated with unsaturated conditions. Miscible displacement equations based on first order exchange of solute between mobile and immobile phases initially discussed by Coats and Smith (1964) were extended by van Genuchten and Wierenga (1976) to include Freundlich type equilibrium adsorption-desorption processes. Their equations are

$$\theta_m R_m \frac{\partial C_m}{\partial t} + \theta_{im} R_{im} \frac{\partial C_{im}}{\partial t} = \theta_m D_a \frac{\partial^2 C_m}{\partial z^2} - \theta_m v_m \frac{\partial C_m}{\partial z} \quad (9.48)$$

$$\theta_{im} R_{im} \frac{\partial C_{im}}{\partial t} = \alpha (C_m - C_{im})$$

where the subscripts  $m$  and  $im$  refer to the mobile and immobile phases, respectively. The retardation factors account for equilibrium type adsorption processes similar to that in (9.46) while the mass transfer coefficient  $\alpha$  embraces a diffusion coefficient and an average diffusional path length. Although (9.48) was used successfully by van Genuchten and Wierenga and by Gaudet et al. (1977) as well as many others more recently to describe laboratory column studies, its use in structured field soils has been limited owing to the difficulty of obtaining reliable values of  $\alpha$  which depend upon the geometry of the soil pore structure (van Genuchten, 1985). For laboratory experiments, the value of  $\alpha$  may well be confounded with nonlinear isotherm and chemically kinetic exchange effects. Moreover, the fraction of  $\theta$  considered to be immobile is sensitive to hysteresis, the concentration of the soil solution, the soil water content and the soil water flux. From the experimental studies of Nkedi-Kizza mentioned earlier in section 9.4.1.4, Fig. 9.21 clearly shows the impact of the solution concentration and the average pore water velocity on the amount of soil water considered to be immobile.

The third formulation considers the first term of (9.38) having two components - one for exchange sites (type 1) on a fraction of the soil particle surfaces that involve instantaneous, equilibrium reactions and another for type 2 exchange sites involving first order kinetics or those assumed to be time-dependent (Selim et al., 1976; Cameron and Klute, 1977). Following Nkedi-Kizza et al. (1984) we have

$$(1 + F\rho_T k\theta^{-1}) \frac{\partial C}{\partial t} + \rho_T \theta^{-1} \frac{\partial C_{s_2}}{\partial t} = D_a \frac{\partial^2 C}{\partial z^2} - v \frac{\partial C}{\partial z} \quad (9.49)$$

$$\frac{\partial C_{s_2}}{\partial t} = \alpha [(1-F)kC - C_{s_2}]$$

where  $F$  is the mass fraction of all sites being occupied with type 1 sites, and where subscript 2 refers to type 2 sites. With values of  $\alpha$  and  $F$  usually being dependent upon the average displacement velocity  $v$ , values of  $F$  appropriate for (9.49) cannot be obtained from equilibrium batch studies. The use of an

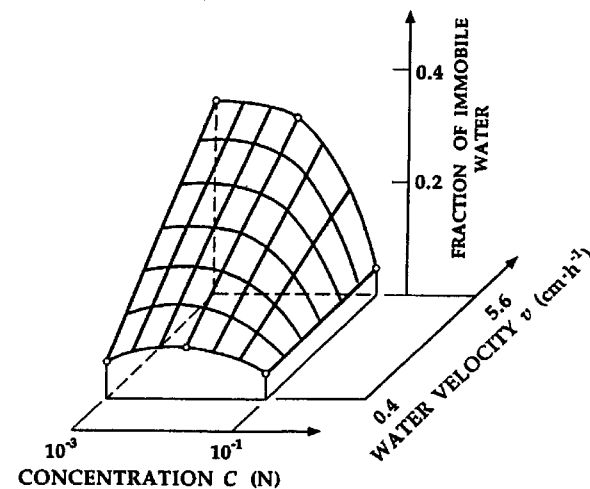


Figure 9.21. Fraction of immobile water versus solute concentration and average pore water velocity.

average value of  $v$  masks any effect of the microscopic pore water velocity distribution on the exchange process.

Comparison of (9.48) and (9.49) shows that they can be put in the same dimensionless form by means of equation-specific dimensionless parameters. With this information Nkedi-Kizza et al. (1984) proved that effluent curves from laboratory soil columns alone cannot be used to differentiate between the specific physical and chemical phenomena that cause an apparent non equilibrium situation during miscible displacement. The similarity of the two sets of equations allows an oftentimes satisfactory empirical description of the mixing of solutes at the macroscopic scale by either equation without ascertaining the exact nature of the particular chemical or physical process at the microscopic scale. The exact nature of the processes awaits further research using micro tomography or other techniques of observation at the microscopic scale.

### 9.5.1.3 Dual-Porosity Models for Structured Soils

Dual porosity models (also called bi-modal porosity models) assume that a soil can be separated into two distinct pore systems superpositioned over the same

soil volume with each system being a homogeneous medium having its own water and solute transport properties (Dykhuizen, 1987). We assume that the same type of mathematical expressions can be used to describe both systems of pores inasmuch as similar capillary effects take place in the pores of both systems (Othmer et al., 1991). With the two systems exchanging water and solutes in response to hydraulic and concentration gradients, the soil is characterized by two water velocities, two hydraulic heads, two water contents and two solute concentrations. Gerke and van Genuchten (1993) provide a comprehensive review of various theoretical and experimental attempts to deal with water and solute movement in saturated and unsaturated structured soils during steady and transient water flow conditions. The basis of their numerical simulations demonstrating the complicated nature of solute leaching in structured, unsaturated soils during transient water flow are summarized here to provide future opportunities for field research in soil hydrology.

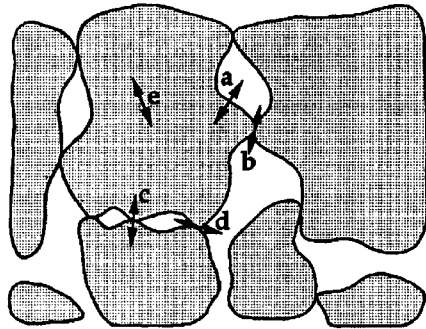


Figure 9.22. Schematic diagram of a structured soil at the microscopic level. Macropores, interaggregate pores and fracture pores appear between shaded areas representing soil aggregates. Arrows represent water and solute movement through a. the surface of an aggregate, through b. the fracture pore, between c. aggregates, between d. continuous and stagnant pores and inside e. an aggregate.

Microscopically, a structured soil (see Fig. 9.22 and our discussion in sections 2.4, 4.3.3 and 5.3.2) consists of soil aggregates (shaded irregular areas) surrounded by inter-aggregate pores (dotted areas) which form a more or less continuous network. The pore network is geometrically a combination of inter-aggregate and intra-aggregate pores further complicated by the presence of distinct mineral and organic particles discussed earlier. Here we use subscript  $M$  to denote the inter-aggregate system and subscript  $m$  to denote the intra-

aggregate system. We refer the reader to the original article of Gerke and van Genuchten (1993) for a complete description of the hydraulic properties of the structured soil and the details of the solute transport equations only briefly described here.

Solute transport with linear adsorption and first order decay is described by

$$\frac{\partial(\theta_M R_M C_M)}{\partial t} = \frac{\partial}{\partial z} \left( \theta_M D_{a_M} \frac{\partial C_M}{\partial z} - q_M C_M \right) - \theta_M \mu_M C_M - \frac{\Gamma_s}{w_M} \quad (9.50)$$

$$\frac{\partial(\theta_m R_m C_m)}{\partial t} = \frac{\partial}{\partial z} \left( \theta_m D_{a_m} \frac{\partial C_m}{\partial z} - q_m C_m \right) - \theta_m \mu_m C_m + \frac{\Gamma_s}{1-w_M}$$

where  $\mu$  is a first order decay coefficient,  $\Gamma_s$  a solute mass transfer term to which both molecular diffusion and convective transport contributes and  $w_M$  is the ratio of the volume of the interaggregate pores to that of the total volume of all pores. With the exception of  $\Gamma_s$  which is defined as the mass of solutes per unit volume of bulk soil per unit time, all variables in (9.50) are defined relative to the partial volume of each pore system.

Although this model and its numerical solution can simulate transport related to specific chemical and physical properties of the soil, its large number of parameters not easily measured experimentally remain a topic of future laboratory and field research.

#### 9.5.1.4 Consecutive Convective-Diffusion Equations

Equation (9.39) is oftentimes sequentially repeated when organic or inorganic products are of interest, especially when the products form a consecutive chain of reactions, e. g. for nitrogen (urea  $\rightarrow$   $\text{NH}_4^+$   $\rightarrow$   $\text{NO}_3^-$   $\rightarrow$   $\text{N}_2$ ). In such cases a set of simultaneous equations stemming from (9.39) becomes

$$\frac{\partial(\rho_T C_{s1})}{\partial t} + \frac{\partial(\theta C_1)}{\partial t} = \frac{\partial}{\partial z} \left( D_{a1} \frac{\partial C_1}{\partial z} \right) - \frac{\partial(q C_1)}{\partial z} + \phi_1 \quad (9.51)$$

$$\frac{\partial(\rho_T C_{sj})}{\partial t} + \frac{\partial(\theta C_j)}{\partial t} = \frac{\partial}{\partial z} \left( D_{aj} \frac{\partial C_j}{\partial z} \right) - \frac{\partial(q C_j)}{\partial z} - \phi_{j-1} + \phi_j$$

where  $j = 2, 3, \dots, n$  when  $n$  is the number of species considered in the reaction chain. The equations are linked to each other by their mutual  $\phi_j$  terms. These equations have been applied to consecutive decay reactions of soil nitrogen species (e. g. Cho, 1971; Misra et al., 1974; Starr et al., 1974), organic phosphates (Castro and Rolston, 1977) and pesticides (Bromilow and Leistra, 1980).

We illustrate the application of (9.51) with an investigation conducted by Wagenet et al. (1977) who extended the mathematical analysis of Cho (1971) and the experimental techniques of Mansell et al. (1968) and Misra et al. (1974) to trace the fate of nitrogen applied as a pulse of 95%  $^{15}\text{N}$ -enriched urea fertilizer to an unsaturated soil column during steady state leaching conditions. The concentration of oxygen within the partially air-filled pores was simultaneously controlled at a desired constant value (Wagenet and Starr, 1977). The transport

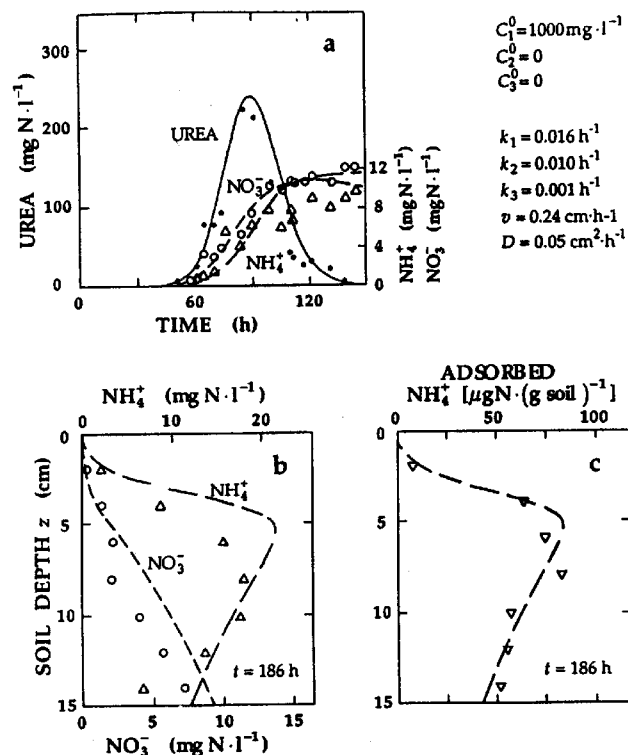


Figure 9.23. Concentration distributions of different nitrogen species identified in the effluent and soil from a pulse of  $^{15}\text{N}$ -enriched urea solution displaced through a column under controlled laboratory conditions.

and transformation of urea,  $\text{NH}_4^+$  and  $\text{NO}_3^-$  were identified by isotopic dilution techniques. Based upon complementary experiments, the enzymatic hydrolysis of urea  $C_1$ , the microbial oxidation of ammonium  $C_2$  and the microbial reduction of nitrate  $C_3$  were each considered first order rate reactions. For their study, (9.51) become

$$\begin{aligned}
 (1+R_1) \frac{\partial C_1}{\partial t} &= D_a \frac{\partial^2 C_1}{\partial z^2} - v \frac{\partial C_1}{\partial z} - k_1 C_1 \\
 (1+R_2) \frac{\partial C_2}{\partial t} &= D_a \frac{\partial^2 C_2}{\partial z^2} - v \frac{\partial C_2}{\partial z} + k_1 C_1 - k_2 C_2 \\
 \frac{\partial C_3}{\partial t} &= D_a \frac{\partial^2 C_3}{\partial z^2} - v \frac{\partial C_3}{\partial z} + k_2 C_2 - k_3 C_3
 \end{aligned}
 \quad (9.52)$$

where  $R_1$  and  $R_2$  are the retardation factors for urea and ammonium [see (9.46)], respectively,  $D_a$  assumed to be identical for each of the chemical species and  $k_1$ ,  $k_2$  and  $k_3$  are the rate constants describing the processes of urea hydrolysis, ammonium oxidation and nitrate reduction, respectively.

Elution curves for the three chemical species identified by the  $^{15}\text{N}$  tracer introduced as a 100-ml pulse of urea solution ( $C_1^0 = 1000 \text{ mg} \cdot \text{l}^{-1}$ ) into a soil column having 20% oxygen in its air-filled pores are shown in Fig. 9.23a. Theoretical and measured concentrations of  $\text{NH}_4^+$ -N and  $\text{NO}_3^-$ -N in the soil solution and those of adsorbed  $\text{NH}_4^+$ -N in the soil column at the conclusion of the displacement process ( $t = 186 \text{ h}$ ) are given in Fig. 9.23b and c, respectively. Details of the methodology to ascertain values of  $v$ ,  $D_a$ ,  $R_1$ ,  $R_2$ ,  $k_1$ ,  $k_2$  and  $k_3$  used in the solutions of (9.50) subject to appropriate initial and boundary conditions are given by Wagenet et al. The rate of nitrification in the presence of 20% oxygen was one order of magnitude greater than that of denitrification. Of the 100 mg  $^{15}\text{N}$  applied to the soil, a mass balance of the  $^{15}\text{N}$  in the chemical species measured in the effluent and in the soil at the conclusion of the experiment was within less than 3 mg.

With consecutive equations such as (9.52), field studies in the presence of higher plants provide opportunities to better understand agro-ecosystems. For example, Mishra and Misra (1993) learned how liming a cultivated field of corn modified the values of  $k_2$  and  $k_3$  as a function of soil depth and time in the presence and absence of crop roots. A better understanding of microbial-induced transformations of other chemical species for transient flow and nonisothermal conditions await investigation in both the laboratory and the field.

### 9.5.2 Chromatographic Formulations

Descriptions of the transport of fluids with their dissolved constituents through beds of reactive porous solids based upon chromatographic plate formulations stem primarily from those derived by chemical engineers nearly one-half century ago (e.g. Wilson, 1940; DeVault, 1943; Thomas, 1944; Glueckauf, 1949; Lapidus and Amundson, 1952; and Heister and Vermeulen, 1952). Subsequent studies in soil hydrology focused first on laboratory soil columns and later were applied in the field for reclaiming saline and sodic soils. For example, to describe cation exchange and ionic distributions within soil columns, Rible and Davis (1955) used DeVault's theory while Bower et al. (1957) used that of Heister and Vermeulen. Van der Molen (1956) predicted the reclamation of saline soils during winter rainfall periods using the theory of Glueckauf. Dutt and Tanji (1962) introduced computer-based chromatographic formulations that were

followed by those of Kovda and Szabolcs (1979) and Oster and Frenkel (1980) which were applied to soil reclamation. Shaffer (1977) extended the model of Dutt to apply to cropped, tile-drained field soils.

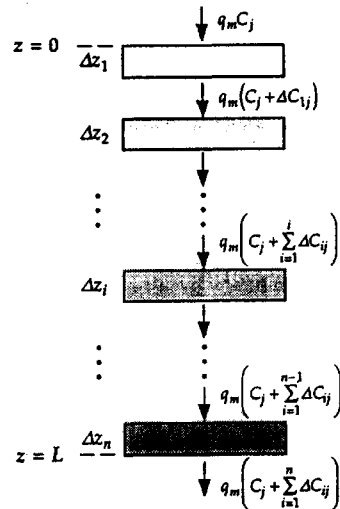


Figure 9.24. Illustration of a chromatographic formulation to describe the displacement and mixing of the soil solution during leaching.

The chromatographic formulation introduced by Dutt and Tanji (1962) is illustrated in Fig. 9.24 where a vertical, homogeneous soil column of length  $L$  of unit cross-sectional area is made up of  $n$  segments (plates) each of length  $\Delta z_i$ . The concentration  $C_j$  of a number of solute species  $j$  entering the column in each leaching aliquot  $\Delta Q_m$  (where  $m$  is the number of the aliquot) changes as the solutes mix, react and pass through each segment. The first aliquot infiltrates into the first segment, and fills it to some prescribed soil water content. The second aliquot of infiltrating water displaces the soil water from the first segment into the second segment, and so forth. If the amount of solution  $\Delta Q$  in each segment  $\Delta z_i$  is identical during infiltration, the final concentration  $C_j^*$  of solute species  $j$  in the first aliquot  $\Delta Q_1$  leached from the column will be

$$C_j^* = C_j + \sum_{i=1}^n \Delta C_{ij} \quad (9.53)$$

where  $\Delta C_{ij}$  is the change in concentration of solute  $j$  when the aliquot  $\Delta Q_1$  is passed through segment  $\Delta z_i$ . As  $n \rightarrow \infty$ , the last term in (9.53) is the integral of the change in solute concentration from  $z = 0$  to  $z = L$ . Assuming that the solution is in chemical equilibrium with the soil in each segment, the difference in concentration between the equilibrium solution and that entering each segment is calculated. If  $n$  in (9.53) is considered finite, the average concentration of the aliquots  $\Delta Q_m$  is calculated by progressively equilibrating the solution of  $\Delta Q_m$  with each of the  $n$  segments assuming that piston flow (Fig. 9.12a) takes place within each segment. The dispersion of the solutes associated with pore water velocity distributions and molecular diffusion are implicitly and empirically included by choosing the number of segments or plates  $n$ . Tanji et al. (1972) utilized the concept of holdback  $H_b$  [see (9.33)] to allow only a fraction of the soil water in each segment to be displaced into the next after chemical equilibrium. They also designated variable segment thicknesses  $\Delta z_i$  corresponding to soil sampling depth intervals or soil horizons as well as choosing the value of  $n$  based upon the dispersion of measured chloride breakthrough curves.

Because transient perturbations of the pore water velocity distribution and soil water content are ignored during infiltration and redistribution, chromatographic formulations of solute transport have more recently emphasized the need to study the kinetic aspects of chemical reactions, exchange processes and dissolution and precipitation. Even when these kinetic aspects have been articulated, the enigma of choosing the number and thickness of the segments to reconcile the omission of the pore water velocity distribution remains the objective of future research.

### 9.5.3 Stochastic Considerations

Because of the naturally occurring heterogeneity of field soils, deterministic formulations of solute transport processes presented above generally must be modified to describe pedon or field scale solute transport. Contemporary research efforts are based upon the consideration that transport phenomena are intrinsically erratic processes susceptible to quantitative characterization by stochastic models. Common to all stochastic models of pedon or field scale transport is the assumption that parameters observed in the field are functions with values distributed in space represented as random variables with discrete values assigned according to a probability distribution. The probability distribution functions at each point in space are usually unknown and cannot be evaluated from only one or a few observations within close proximity of the location. Reviews by Jury (1983) and Dagan (1986) provide pedagogic details. Many other statistical approaches are also described in the literature [e.g. continuous Markov processes (Knighton and Wagenet, 1987), random walk formulations (Kinzelbach, 1988), moment analyses (Cvetkovič, 1991) and hierarchical methods (Wheatcraft and Cushman, 1991)]. Here, we consider three approaches that are available to deal with spatial and temporal variability in addition to the state-space equations previously described in Chapters 7 and 8.

### 9.5.3.1 Monte Carlo Simulations

Monte Carlo simulations of a solution of a deterministic equation such as (9.42) allow coefficients to be random variables of the nature expected within a heterogeneous field soil. The variable may be independent, spatially or temporally correlated and perhaps manifest a variance structure. Based upon an initial sampling, parameters selected for the assumed probability density function (pdf) permit repeated solutions ( $i = 1, 2, \dots$ ) of the deterministic equation [e.g.  $C_i(z, t)$ ] to be calculated. These solutions  $C_i(z, t)$  are then used to calculate sample moments (mean, variance) which are assumed to represent the statistical properties of the underlying stochastic process.

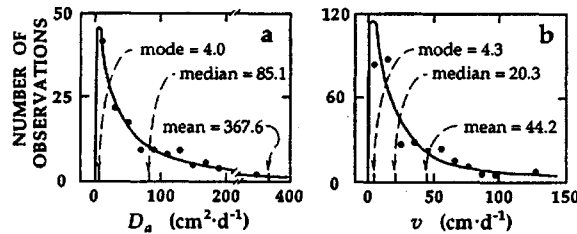


Figure 9.25. Probability distribution functions of  $D_a$  and  $v$  presented in Fig. 9.20.

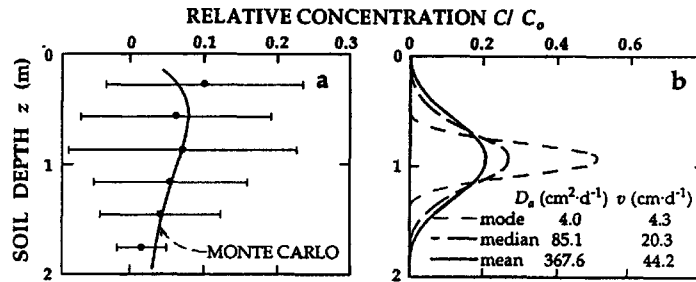


Figure 9.26. Solute concentration distributions within a field soil. a. Monte Carlo simulation and b. Deterministic equation (9.44). Measured values and their standard deviations are represented by solid circles and horizontal bars, respectively.

Amoozgar et al. (1982) relied on the initially measured observations of  $D_a$  and  $v$  shown in Fig. 9.20a and their pdfs shown in Fig. 9.25 together with the normal pdf of  $\theta$  to estimate the solute concentration distribution  $C(z, t)/C_0$  expected at any location within a field. The average solute concentration distribution  $\bar{C}(z, t)/C_0$  expected for the entire field was derived from repeated calculations of (9.44) using the following Monte Carlo step-wise procedure:

1. Draw a random value from the normal distribution with mean zero and standard deviation 1 (Maisei and Gnugnoli, 1972).
2. Find random values of  $\ln D$ ,  $\ln v$  and/or  $\theta$  from their respective statistical distributions represented by the equation  $y = \beta\sigma + \mu$  where  $\beta$  is the value with mean zero and standard deviation 1, and  $y$  is the random value with mean  $\mu$  and standard deviation  $\sigma$ .
3. Calculate the random value of  $C/C_0$  from (9.44) using the above values of  $D_a$ ,  $v$  and  $\theta$  for each  $z$  and  $t$ .
4. Repeat steps 1 through 3 above 2000 times and calculate the mean value of  $C/C_0$  for each  $z$  and  $t$ .

The average solute concentration distribution  $\bar{C}(z, t)/C_0$  expected for the entire field at time  $t = 2$  d for a pulse input of solute concentration  $C_0$  for  $t_1 = 0.4$  d is shown in Fig. 9.26a together with the field values measured by Biggar and Nielsen (1976). Note that these distributions differ markedly from those in Fig. 9.26b calculated from (9.44) using constant values of  $D_a$ ,  $v$  and  $\theta$ . The spreading of the solute averaged over the entire field is dominated by variations in pore water velocity (Bresler and Dagan, 1979, and Dagan and Bresler, 1979).

Two kinds of solute distributions are of interest. The first kind is that of  $C(z, t)/C_0$  realized at any location within a field, and the second is that of  $\bar{C}(z, t)/C_0$  obtained by averaging a large number of  $C_i(z, t)/C_0$  across a field. The former is important because it is associated with a particular soil pedon location, a single crop plant or a small community of plants. With site-specific crop and soil management practices, each location can indeed be treated and managed individually across the entire field in order to account for local variations of soil properties (Robert et al., 1993). The latter is important because it is the expectation of solute retention and emission of solutes from an entire field considered as a single domain. Although there is general appreciation of the latter, a farmer is also appreciative of the former owing to the desire to provide optimum growing conditions for each and every crop plant within the cultivated field.

Present-day research within soil mapping units focusing on auto- and cross-correlation lengths of soil properties and variables [such as those in (9.44)] will eventually allow the delineation of the extent of a field characterized by a single simulation. The opportunities afforded by Monte Carlo simulations hinge upon the development of methods to measure and ascertain pdfs of the transport coefficients within prescribed limits of vadose zone depths and times.

### 9.5.3.2 Stochastic Continuum Equations

Recognizing the paucity of solute concentration data usually available in soils and other subsurface environments coupled with their natural geometric complexities and heterogeneity, Gelhar et al. (1979) initiated stochastic continuum formulations to describe transport processes in water-saturated aquifers. Unlike the above Monte Carlo methods which assume that the random parameters or variables have no spatial correlation, stochastic continuum formulations assume that a random variable can be represented by the sum of its mean and a spatially correlated random fluctuation.

We illustrate the approach with Darcy's equation that describes the mean vertical water flux density  $\bar{q}$  in a saturated soil (5.5) as

$$\bar{q} = -\bar{K}_S \frac{d\bar{H}}{dz} \quad (9.54)$$

where  $\bar{q}$ ,  $\bar{K}_S$  and  $\bar{H}$  are expected mean values. Assuming that the values of  $z$  and its derivative are measurable and known deterministically within desired, prescribed limits of accuracy, (9.54) can be written as

$$q = (\bar{q} + \tilde{q}) = -(\bar{K}_S + \tilde{K}_S) \frac{d(\bar{H} + \tilde{H})}{dz} \quad (9.55)$$

where each of the terms  $\tilde{q}$ ,  $\tilde{K}_S$  and  $\tilde{H}$  are random, spatially autocorrelated functions and have a zero mean value. Subtracting (9.54) from (9.55) yields

$$\tilde{q} = -\bar{K}_S \frac{d\tilde{H}}{dz} - \tilde{K}_S \frac{d\bar{H}}{dz} - \tilde{K}_S \frac{d\tilde{H}}{dz} \quad (9.56)$$

The terms in such an equation evaluated by deriving a first-order equation for the fluctuations are solved with Fourier transforms (Gelhar et al., 1979).

When a random parameter such as  $D_a$  in (9.42) is represented by the sum of its mean value and a random fluctuation, a mean transport model with additional terms is obtained. By solving the stochastic equation of the local-scale water and solute transport, the functional form of  $D_a$  for macroregions is related to the statistics describing the variability. A macro-scale value of  $D_a$  is reached asymptotically as distance and/or time increase. From such an analysis the long-term, large-scale solute transport can be described using the stochastically derived value of  $D_a$  in the deterministic equation (9.42).

A limited number of field aquifer experiments (e.g. Sudicky et al. 1985, and Freyberg, 1986) have shown that the value of  $D_a$  increases with solute travel time and travel distance and gradually approaches a constant asymptote consistent with the analysis proposed by Gelhar et al. The application of stochastic continuum research for unsaturated soils appears promising (e.g. Russo, 1993, and Yeh et al., 1985a, b and c) but not yet sufficiently developed to be a proven field technology.

## 9.5 Theoretical descriptions

### 9.5.3.3 Stochastic Convective Equations

The displacement and attenuation of a solute distribution within a vertical soil profile during infiltration can be considered the result of a stochastic convective flow process with its formulation based upon a solute travel time probability density function. The advantage of such formulations is that they do not require an explicit accounting of all of the various physical, chemical and biological processes occurring in the complex, heterogeneous soil environment. Although many stochastic convective models have been used in different scientific disciplines, those initiated by Simmons (1982) and Jury (1982) stimulated research in soil hydrology during the past decade. Here we introduce the stochastic convective concept as a transfer function (Jury, 1982) which can easily be obtained for a nonreactive solute by a single, simple field calibration to measure the travel time distribution. It is assumed that no dispersion of the solute takes place other than that which is represented by the travel time variations within the soil.

Assuming that the depth reached by a solute applied in water at the soil surface depends upon the net amount of water applied, the probability that the solute will reach depth  $L$  after a net amount of water  $I$  has been applied to the soil surface is

$$P_L(I) = \int_0^I f_L(I') dI' \quad (9.57)$$

where  $f_L(I)$  is the probability density function.  $f_L(I)$  is the average concentration at soil depth  $z = L$  in response to a narrow pulse (Dirac  $\delta$ -function) of solute  $C_{IN} = C_0 \delta(I)$  applied at  $I = 0$  at the soil surface. A set of observations of  $f_L(I)$  can be obtained by measuring the soil solution concentration at depth  $L$  at various locations within a field to determine the amount of uniformly applied water  $I$  required to move the solute pulse from the soil surface to depth  $L$ . The average concentration  $C_L(I)$  at  $z = L$  for arbitrary variations of solute  $C_{IN}$  applied at the soil surface is

$$C_L(I) = \int_0^I C_{IN}(I - I') F_L(I') dI' \quad (9.58)$$

The integrand is the probability  $f_L(I')$  of reaching  $z = L$  between  $I'$  and  $(I' + dI')$ , and multiplied by the concentration  $C_{IN}(I - I')$  of solution displacing at  $I'$ . For spatially variable water application rates Jury used a joint probability function in (9.58).

We assume that the distribution of physical processes contributing to the probability density  $f_L(I)$  between  $z = 0$  and  $z = L$  is the same for all soil depths. Hence the probability that an applied solute will reach any depth  $z$  after an amount of water  $I = I_1$  has infiltrated the soil surface is equal to the probability of reaching  $z = L$  after  $I = I_1 L z^{-1}$  has infiltrated. For example, the probability of reaching a depth of 50 cm with 10 cm of infiltrated water is equal to the probability of reaching 100 cm with 20 cm of infiltrated water. Hence, from (9.57)

$$P_z(I) = P_L\left(\frac{IL}{z}\right) = \int_0^{ILz^{-1}} f_L(I') dI' \quad (9.59)$$

To predict the average solute concentration as a function of any depth  $z \neq L$ , we relate the probability density function  $f_z(I)$  to the reference density function  $f_L$  by

$$f_z(t) = \frac{L}{z} f_L\left(\frac{Lt}{z}\right) \quad (9.60)$$

and obtain

$$C(z, t) = \int_0^{\infty} C_{IN}(1-t') \frac{L}{z} f_L\left(\frac{t'L}{z}\right) dt' \quad (9.61)$$

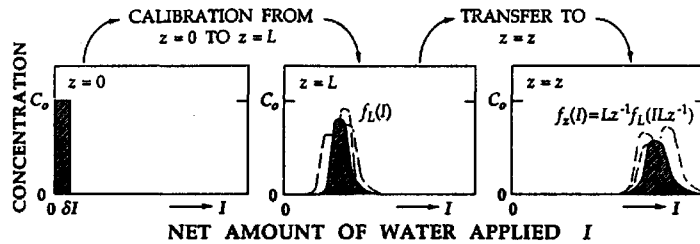


Figure 9.27. The concept of a transfer function calibrated at depth  $L$  to predict the arrival of a solute pulse from the soil surface at depth  $z$  as a function of the net amount of water applied at the soil surface. The broken curves each represent a distribution measured at a specific location within the field.

The concept is illustrated in Fig. 9.27 where the broken lines in the graphs for  $z = L$  and  $z = z$  represent concentration distributions measured at individual locations within the field.

If the transport properties are statistically similar for all depths, only one calibration  $f_L$  is needed. On the other hand, if they are dissimilar owing to strongly developed horizons or textural and structural differences, additional calibrations  $f$  are required or a more robust calibration  $f_L$  for all depths can be made at depth  $L$  below the strongly stratified soil.

Relatively few distributions of solute transport parameters have been measured in the field. Some of them appear to be lognormal. For such distributions the travel time density function  $f_z(t)$  is

$$f_L(t) = \left[ \frac{1}{(2\pi)^{1/2} \sigma t} \right] \exp \left[ \frac{-(\ln t - \mu)^2}{2\sigma^2} \right] \quad (9.62)$$

where  $\mu$  is the mean of the distribution of  $\ln t$  and  $\sigma^2$  the corresponding variance. On the other hand (9.44) for the same boundary and initial conditions yields the travel time density function  $f_z(t)$

$$f_L(t) = \left[ \frac{L}{2(\pi D_a t^3)^{1/2}} \right] \exp \left[ \frac{-(L - vt)^2}{4D_a t} \right] \quad (9.63)$$

Although the above functions are nearly identical when calibrated at the same

depth (Simmons, 1982), they yield distinctly different predictions of solute movement at depths  $z \neq L$ . Jury and Sposito (1985) have shown that the variances of the travel time for (9.62) and (9.63) are

$$\text{var}_{z_{TM}}[t] = z^2 L^{-2} \exp(2\mu) \left\{ \exp(2\sigma^2) - \exp(\sigma^2) \right\} \quad (9.64)$$

and

$$\text{var}_{z_{COE}}[t] = 2Dz v^{-3}, \quad (9.65)$$

respectively. Inasmuch as  $\text{var}_{z_{TM}}[t]$  increases as the square of the depth  $z$  while that of (9.44) increases linearly with depth, the lognormal transfer function model predicts the greater amount of solute spreading for the same depth. Present-day field experimentation for different soils and local conditions is sufficiently limited to preclude a preferred choice of the two models (e.g. see Jury and Sposito, 1985).

Presently, stochastic-convective formulations are being extended to include the transport of adsorbing and decaying solutes, two component chemical nonequilibrium models, physical nonequilibrium models and other nonlinear processes. See a review by Sardin et al. (1991) as well as a more recent contribution by Roth and Jury (1993).

## 9.6 IMPLICATIONS FOR WATER AND SOLUTE MANAGEMENT

Although our understanding and theoretical description of solute transport in soils remain incomplete, we have nevertheless sufficient knowledge to derive a few principles or guidelines for managing solute retention or leaching in the field. Whether solutes accumulate or leach depends primarily upon the processes by which they enter, react and leave the soil profile relative to their association with water. Here, we make no attempt to discuss the well-known principles of managing salinity and drainage from irrigated agricultural lands used for crop production inasmuch as excellent texts are abundantly available. Disregarding horizontal surface and subsurface water flow, we focus our attention on transport owing to the water content and flux density conditions at the soil surface occurring naturally owing to local weather conditions and being deliberately modified by irrigation.

Summarizing the more important points of this chapter, we conclude the following regarding the relative movements of soil water and its dissolved constituents:

- As water moves more slowly through a soil, there is a greater opportunity for more complete mixing and chemical reactions to take place within the entire microscopic pore structure owing to the relative importance of molecular diffusion compared with that of convection.
- Microscopic pore water velocity distributions manifest their greatest divergence for water-saturated soil conditions. Hence, under water-saturated conditions, the greatest proportion of water moving through the soil matrix occurs within the largest pore sequences.

- c. Under water-saturated soil conditions, when the average pore water velocity is large compared with transport by molecular diffusion, the relative amount of solute being displaced depends upon the solute concentration of the invading water.
- d. The concept of preferential flow paths occurs at all degrees of water-unsaturation even though their existence is usually only demonstrated for macropores near water-saturation. At each progressively smaller water content, the larger pore sequences remaining full of water establish still another set of preferential flow paths.
- e. Any attempt to measure the solute concentration based on extraction methods carried out either in the laboratory or the field will be dependent upon the rate of extraction and the soil water content during the extraction process.
- f. Inasmuch as rainfall infiltration usually occurs at greater soil water contents and greater average pore water velocities than does evaporation at the soil surface, the amount of solutes transported near the soil surface per unit water moving through the soil surface is greater for evaporation than for infiltration.

Each of the above six points have been verified one way or another in numerous publications before and after the observations made in a field experiment conducted by Miller et al. (1965) which we describe below.

A level 0.4-ha site of Panoche clay loam was divided into 0.004-ha plots statistically replicated in five complete blocks. Potassium chloride uniformly applied to the soil surface was leached and redistributed within the profile with four different methods of water application: a. the soil surface continuously ponded with water, b. the soil surface intermittently ponded with repeated applications of 15-cm of water, c. the soil surface intermittently ponded with repeated applications of 5-cm of water and d. the soil surface continuously sprinkled at a rate less than  $K_s$  and equal to  $0.3 \text{ cm}\cdot\text{h}^{-1}$ . The intermittent applications were made weekly when the soil water pressure head at the 30-cm soil depth reached a value of  $-150 \text{ cm}$ . Each method gave rise to different soil water content distributions  $\theta(z,t)$  and different water flux density distributions  $q(z,t)$ . Average values  $\bar{\theta}(z,t)$  and  $\bar{q}(z,t)$  for each method were a. 0.48 and 0.6, b. 0.44 and 0.09, c. 0.42 and 0.03 and d.  $0.42 \text{ cm}^3\cdot\text{cm}^{-3}$  and  $0.3 \text{ cm}\cdot\text{h}^{-1}$ , respectively. Soil solution samples taken every 30 cm to a depth of 150 cm were frequently extracted and analyzed in the laboratory for their chloride content. From the five plots of each treatment about 3500 samples were analyzed. Additional details regarding the exact nature of the infiltration, redistribution and soil water content profiles are available (Nielsen et al., 1967).

The chloride concentration distributions from the four water application methods manifest significant differences (Fig. 9.28). Although some chloride leached to great depths in the continuously ponded soil after 15 cm water had infiltrated, most all of the solute resided in the top 50 cm of soil. In the other three treatments for the same amount of water infiltrated, large quantities of the solute had been dispersed twice the depth to 100 cm. For 60 cm of infiltration, the center of the solute mass is displaced to greater depths as  $\bar{\theta}(z,t)$  decreases.

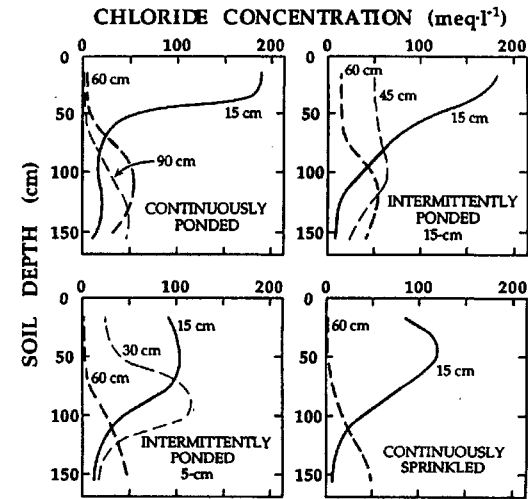


Figure 9.28. Field-measured chloride concentration distributions from a surface application of potassium chloride being leached through the profile as a result of four different water application treatments. Values associated with each curve correspond to cumulative amounts of water infiltrated

That is, for the continuously ponded case, the relative maximum chloride concentration is just below 100 cm while those for the intermittent 5-cm ponding and for continuous sprinkling were both below 150 cm. Indeed, the concentration of solute for the latter two treatments for 60 cm of water infiltrated is everywhere less than that of the continuously ponded case when as much as 90 cm of water had infiltrated. Under the continuously ponded condition, judging the small solute concentration to a depth of 90 cm when a depth of 90 cm of water had been applied, its behavior conformed to the recommendation, "It takes a cm of water to leach a cm of soil". Here we note that for unsaturated, slow leaching conditions, it took only 60 cm of water to leach the same amount of solute as was required for 90 cm of water under near-saturated ponded conditions. The distribution curves for intermittent 5-cm ponding and for continuous sprinkling are remarkably similar. Even though their values of  $\bar{q}(z,t)$  differed by one order of magnitude, at such slow flow rates relative differences in mixing by molecular diffusion are apparently insignificant to the spreading of solute at nearly identical  $\bar{\theta}(z,t)$ .

Two additional comments are appropriate for the data presented in Fig. 28. First, consider the 15-cm curve for continuous ponding, the 45-cm curve

for 15-cm intermittent ponding and the 30-cm curve for 5-cm intermittent ponding. If we assume that a nitrate fertilizer instead of a chloride salt had been applied to the soil surface, three entirely different solute distributions could have achieved different purposes. For continuous ponding, the fertilizer is leached in a concentrated solution for the benefit of a shallow-rooted crop. For 5-cm intermittent ponding, fertilizer is leached to the roots of a deep-rooted crop (e.g. a fruit tree crop) and not in the vicinity of an associated, shallow-rooted cover crop. The 45-cm curve for 15-cm intermittent ponding illustrates uniform fertilization to a 125-cm soil depth – a desired result for both deeper-rooted and shallow-rooted crops growing in the same community. Second, consider the curves for continuous ponding and those for 5-cm intermittent ponding. If we assume that a chlorinated pesticide moves approximately like chloride and has a lethal dose equivalent to  $100 \text{ meq}\cdot\text{l}^{-1}$  chloride, we note that pests such as nematodes are killed to a depth greater than 100 cm if we leach the pesticide with intermittent ponding. On the other hand, by adding the same quantity of pesticide to the soil surface and leaching it under continuously ponded conditions, nematodes thrive at depths below 60 cm.

Although the solute distributions and their interpretations above support many of the six points made in this section, they remain empirical and speculative owing to the fact that such distributions cannot at this time be accurately predicted based upon our present knowledge of soil hydrology. Different results will no doubt be obtained for different soils, solutes and local conditions. Even for the above experiment, had the intermittent applications of water been made at intervals greater than one week, entirely different results would have occurred. That is, it is known based upon the analysis of the soil water behavior in this study (Nielsen et al., 1967) that at the end of one week, evaporation at the soil surface together with gravitational redistribution of soil water allowed a net vertically upward movement of water from the 90-cm soil depth. Hence, at those smaller soil water contents and water flux densities, the chloride would have started to move more efficiently to the soil surface. In such a case, continually ponding the soil surface would have more efficiently leached the soluble solute per unit water infiltrated from the 150-cm soil profile.

Fig. 9.29 shows an example of the chloride concentrations measured within the soil profiles from which the distributions given in Fig. 9.28 were derived. The figure pertains to the intermittently 15-cm ponded treatment for soil depths of 30, 90 and 150 cm. A distinctive characteristic of the curves for the 30- and 90-cm depths is the relative minimum reached soon after the initiation of each 15-cm water application. Similarly, a relative maximum is reached near 400 h soon after the third 15-cm water application. This behavior is associated with the sampling technique. When soil solution is extracted, the bulk of the flow takes place in the larger water-filled pore sequences. Hence, at the shallower depths, the more solute-free infiltrating water flowing through the larger water-filled pores and extracted by the soil solution samplers during infiltration yields a solution that is, indeed, more dilute than the average solute concentration at that depth. Similarly, the more concentrated solution from the shallower depths temporarily taken into the soil solution samplers at the greater depth is greater than the average solute concentration at that depth.

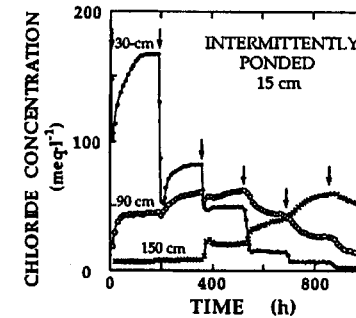


Figure 9.29. Chloride concentration distributions measured at depths of 30, 90 and 150 cm. Zero time represents the time when the first 15-cm ponded water application was initiated. The vertical arrows indicate the other times when additional 15-cm applications were initiated.

Acknowledging that the efficiency of solute leaching obeys the principles discussed here, Dahiya et al. (1985) nevertheless recommend that leaching of saline soils be carried out under continuously ponded conditions based upon their experiments with different plot sizes. They argue that under practical situations in which reclamation is carried out in large field domains, controlled slower, uniform infiltration at smaller soil water contents would require more labor and time.

Except for the post script that follows, we conclude our book with the admonishment that observations and theories of soil hydrology have not yet completely reconciled different scales of space and time in the management of fresh water retained at continental surfaces.

## PROBLEMS

1. Considering a soil column in the laboratory to be equivalent to a bundle of independent capillary tubes, calculate breakthrough curves similar to that shown in Fig. 9.5b for a. a column composed of equal-sized capillary tubes and b. a column composed of two tubes of radius 0.1 cm and 4000 tubes of radius 0.001 cm. Discuss your answer in terms of "preferential flow".
2. By changing variables ( $X, t$ ) of (9.24) to  $[(z - vt), t]$  and substituting  $D_a$  for  $D$ , derive (9.42).
3. Assume that (9.44) describes a pulse of solute ( $t_1 = 0.4$  d) being leached through a homogeneous, water-saturated soil column of length 2 m. For an average pore water velocity  $v = 40 \text{ cm}\cdot\text{d}^{-1}$ , you measured at  $z = 1$  m a

relative maximum concentration  $[(C - C_i)(C_o - C_i)^{-1}] = 0.22$ . What is the value of  $D_a$ ? Hint: First obtain  $\partial C / \partial z$  and set it equal to zero.

3. a. Experimentally for the above problem, how could you best establish the boundary condition  $C = C_o$   $[0, (0 < t \leq t_1)]$ ? b. Similarly, how could you best experimentally establish the constant solute flux density boundary condition  $[vC - D_a \partial C / \partial z = \text{constant}]$  at  $z = 0$ ? In each case, explain the limitations of alternative techniques.
4. Show that for large values of  $v D_a^{-1}$ , (9.44) reduces to

$$\frac{C - C_i}{C_o - C_i} = \frac{1}{2} \left\{ \operatorname{erfc} \left[ \frac{z - vt}{(4D_a t)^{1/2}} \right] - \operatorname{erfc} \left[ \frac{z - v(t - t_1)}{(4D_a(t - t_1))^{1/2}} \right] \right\}$$

Hint:  $\lim_{x \rightarrow \infty} \exp(x) \operatorname{erfc}(x) = 0$ .

5. You are interested in simulating with (9.44) the spreading of a solute pulse (initially of thickness  $vt_1 = 15$  cm in the topsoil) moving below plant roots in the vadose zone of a semi-arid environment. The long-term average net amount of water moving past the zero flux plane in the soil profile is only  $0.01 \text{ cm} \cdot \text{d}^{-1}$ . You first assumed that  $D_c \gg D_m$  and approximated  $D_a$  in (9.44) by  $\beta v$  using a published field-estimated value of the dispersivity  $\beta = 3$  cm. Next, you assumed that  $D_c = D_m = 0.6 \text{ cm}^2 \cdot \text{d}^{-1}$ .
- a. With your first assumption, calculate the distribution of the solute  $\{[C(z) - C_i][C_o - C_i]^{-1}\}$  in the vadose zone for times  $t = 100$  and  $1000$  y. b. With your second assumption, calculate the distribution of the solute  $\{[C(z) - C_i][C_o - C_i]^{-1}\}$  in the vadose zone for the same times. Which assumption do you believe is more realistic, and why?
6. Discuss the implications of using temporal and spatial average values of  $D_a$  and  $v$  in the above problem.
7. The term  $\phi_i$  in (9.35) sometimes represents the growth of soil microbes with the Michaelis-Menten process having the form

$$\phi_i = \frac{\kappa_m C}{K_m + C}$$

where  $\kappa_m$  is the product of a maximum growth rate constant and the biomass of the microbes and  $K_m$  is a "saturation" constant. a. For a concentrated soil solution, show that the above equation reduces to a zero-order equation with a constant value  $\phi = k_o$ . b. For a dilute soil solution, show that the above equation reduces to a first-order equation with  $\phi = kC$  as was assumed in (9.52).

## REFERENCES

- Amanthakrishnan, V., W.N. Gill and A.J. Barduhn. 1965. Laminar dispersion in capillaries: Part I. Mathematical Analysis. *Am. Inst. Chem. Eng. J.* 11:1063-1072.
- Amoozegar, A., D.R. Nielsen and A.W. Warrick. 1982. Soil solute concentration distributions for spatially varying pore water velocities and apparent diffusion coefficients. *Soil Sci. Soc. Am. J.* 46:3-9.
- Aris, R. 1956. On the dispersion of a solute in a fluid flowing through a tube. *Proc. Roy. Soc. London A.* 235:67-77.
- Bazin, M.J., P.T. Saunders and J.I. Prosser. 1976. Models of microbial interactions in the soil. *Chemical Rubber Co. (CRC) Crit. Rev. Microbiol.* 5:464-497.
- Bear, J. 1969. Hydrodynamic dispersion. In: R.J.M. De Wiest (Ed.): *Flow through porous media*, Academic Press, New York and London.
- Bear, J. and Y. Bachmat. 1967. A generalized theory of hydrodynamic dispersion in porous media. *Proc. Intl. Assoc. Sci. Hydrol. Symp. Haifa, Publ. No. 72.*
- Biggar, J.W. and D.R. Nielsen. 1961. Measuring capillary conductivity. *Soil Sci.* 92:192-193.
- Biggar, J.W. and D.R. Nielsen. 1976. Spatial variability of the leaching characteristics of a field soil. *Water Resour. Res.* 12:78-84.
- Bird, R.B., W.E. Stewart and E.N. Lightfoot. 1960. *Transport Phenomena*. Wiley, New York.
- Bolt, G.H. (Ed.). 1979. *Soil Chemistry, Physico-Chemical Models*. Elsevier Science, New York.
- Bosworth, R.C.L. 1948. Distribution of reaction times for laminar flow in cylindrical reactors. *Phil. Mag.* 39:847-862.
- Bower, C.A., W.R. Gardner and J.O. Goertzen. 1957. Dynamics of cation exchange in soil columns. *Soil Sci. Soc. Am. Proc.* 21:20-24.
- Bresler, E. and G. Dagan. 1979. Solute dispersion in unsaturated heterogeneous soil at field scale: II. Applications. *Soil Sci. Soc. Am. J.* 43:467-472.
- Brigham, W.E., P.W. Reed and J.N. Dew. 1961. Experiments on mixing during miscible displacement in porous media. *Soc. Petrol. Engrs. J.* 1:1-8.
- Cameron, D.A. and A. Klute. 1977. Convective-dispersive solute transport with a combined equilibrium and kinetic adsorption model. *Water Resour. Res.* 13:183-188.
- Castro, C.L. and D.E. Rolston. 1977. Organic phosphate transport and hydrolysis in soil: Theoretical and experimental evaluation. *Soil Sci. Soc. Am. J.* 41:1085-1092.
- Cho, C.M. 1971. Convective transport of ammonium with nitrification in soil. *Can. J. Soil Sci.* 51:339-350.
- Coats, K.H. and B.D. Smith. 1964. Dead-end pore volume and dispersion in porous media. *Soc. Petrol. Engrs. J.* 4:73-84.
- Corey, J.C., D.R. Nielsen and J.W. Biggar. 1963. Miscible displacement in saturated and unsaturated sandstone. *Soil Sci. Soc. Am. Proc.* 27:258-262.
- Crank, J. 1956. *The Mathematics of Diffusion*. Oxford Univ. Press, London.
- Currie, J.A. 1960. Gaseous diffusion in porous media. II. *Brit. J. Appl. Phys.* 11:314-324.

- Cvetkovič, V.D. 1991. mass arrival of reactive solute in single fractures. *Water Resour. Res.* 27:177-183.
- Dagan, G. 1986. Statistical theory of groundwater flow and transport: Pore to laboratory, laboratory to formation and formation to regional scale. *Water Resour. Res.* 22:102-135.
- Dagan, G. and E. Bresler. 1979. Solute dispersion in unsaturated heterogenous soil at field scale: I. Theory. *Soil Sci. Soc. Am. J.* 43:461-467.
- Dahiya, I.S., K.S. Grewal, R. Anlauf and J. Richter. 1985. Desalinization of a salt-affected soil in plots of various sizes under two modes of water application. *J. Agric. Sci., Camb.* 104:19-26.
- Danckwerts, P.V. 1953. Continuous flow systems. *Chem. Eng. Sci.* 2:1-13.
- Davidson, J.M. and J.R. McDougal. 1973. Experimental and predicted movement of three herbicides in water-saturated soil. *J. Environ. Qual.* 2:428-433.
- Davidson, J.M., D.R. Nielsen and J.W. Biggar. 1966. The dependency of soil water uptake and release upon the applied pressure increment. *Soil Sci. Soc. Am. Proc.* 30:298-304.
- Day, P.R. 1956. Dispersion of a moving salt water boundary advancing through a saturated sand. *Trans Am. Geophys. Union* 37:595-601.
- de Josselin de Jong, G. 1958. Longitudinal and transverse diffusion in granular deposits. *Trans Am. Geophys. Union* 39:67-74.
- De Vault, D. 1943. The theory of chromatography. *J. Am. Chem. Soc.* 65:534-540.
- Dutt, G.R. and P.F. Low. 1962. Diffusion of alkali chlorides in clay-water systems. *Soil Sci.* 93:233-240.
- Dutt, G.R. and K.K. Tanji. 1962. Predicting concentrations of solutes percolated through a column of soil. *J. Geophys. Res.* 67:3437-3439.
- Dykhuizen, R.C. 1987. Transport of solutes through unsaturated fractured media. *Water Research* 21:1531-1539.
- Freeze, R.A. and J.A. Cherry. 1979. *Groundwater*. Prentice-Hall, Inc., Englewood, New Jersey.
- Freyberg, D.L. 1986. A natural gradient experiment on solute transport in a sand aquifer, 2. Spatial moments and the advection and dispersion of non-reactive solutes. *Water Resour. Res.* 22:3031-2046.
- Fried, J.J. and M.A. Combarous. 1971. Dispersion in porous media. *Advances Hydrosci.* 7:169-282.
- Gaudet, J.P., H. Jegat, G. Vachaud and P.J. Wierenga. 1977. Solute transfer with diffusion between mobile and stagnant water through unsaturated sand. *Soil Sci. Soc. Am. J.* 41:665-671.
- Gelhar, L.W., A.L. Gutjahr and R.L. Naff. 1979. Stochastic analysis of macrodispersion in aquifers. *Water Resour. Res.* 15:1387-1397.
- Gerke, H.H. and M.Th. van Genuchten. 1993. A dual-porosity model for simulating the preferential movement of water and solutes in structured porous media. *Water Resour. Res.* 29:305-319.
- Glueckauf, E. 1949. The theory of chromatography, Part VI. Precision measurements of adsorption and exchange isotherms from column-elution data. *J. Chem. Soc.* 4:3280-3285.
- Gouy, C. 1910. Sur le construction de la charge électrique à la surface d'un électrolyte. *J. de Physique* 9:657-668.
- Gutjahr, A. 1985. Spatial variability: Geostatistical methods. In: D.R. Nielsen and J. Bouma (Eds.): *Soil Spatial Variability*. Pudoc, Wageningen, p. 9-34.
- Heister, N.K. and T. Vermuelen. 1952. Saturation performance of ion exchange and adsorption columns. *Chem. Eng. Prog.* 48:505-516.
- Helferich, F. 1962. *Ion Exchange*. Advances in Chemistry Series. McGraw-Hill, New York.
- Jackson, R.D., D.R. Nielsen and F.S. Nakayama. 1963. On diffusion laws applied to porous materials. *U.S. Dept. Agr. ARS* 41-86.
- Javandel, J., C. Doughty, Chin-Fu Tsang. 1984. *Groundwater transport: Handbook of Mathematical Models*. Amer. Geophys. Union, Washington, D.C.
- Journel, A.G. and C.J. Huijbregts. 1978. *Mining Geostatistics*. Academic Press, New York.
- Jury, W.A. 1982. Simulation of solute transport with a transfer function model. *Water Resour. Res.* 18:363-368.
- Jury, W.A. 1983. Chemical transport modeling: Current approaches and unresolved problems. In: SSSA Special Publication No. 11, SSSA and ASA, Madison, Wisconsin, p. 49-64.
- Jury, W.A. 1989. Spatial variability of soil properties. In: S.C. Hern and S.M. Melancon (Eds.): *Vadose Zone Modeling of Organic Pollutants*. Lewis Publishers, p. 245-269.
- Jury, W.A. and G. Sposito. 1985. Field calibration and validation of solute transport models for the unsaturated zone. *Soil Sci. Soc. Am. J.* 49:1331-1341.
- Kemper, W.D. 1960. Water and ion movement in thin films as influenced by the electrostatic charge and diffuse layer of cations associated with clay mineral surfaces. *Soil Sci. Soc. Am. Proc.* 24:10-16.
- Kinzelbach, W. 1988. The random walk method in pollutant transport simulation. In: E. Custodio, A. Gurgui and J.P. Lobo Ferreira (eds.). *Groundwater Flow and Quality Monitoring*. D. Reidel, Hingham, MA, p. 227-246.
- Knighton, R.E. and R.J. Wagenet. 1987. Simulation of solute transport using a continuous time Markov process. 2. Application to transient field conditions. *Water Resour. Res.* 23:1917-1925.
- Kolmogorov, A.N. 1941. Interpolated and extrapolated stationary random sequences (in Russian). *Izvestia Akademii Nauk SSSR, seriya matematicheskaya* 5 (1).
- Kovda, V.A. and I. Scabolts. 1979. Modeling of soil salinization and alkalization. *Agrokem. Talajt.* 28:1-208.
- Krige, D.G. 1966. Two-dimensional weighted moving average trend surfaces for ore-evaluation. *J. South African Inst. Mining Metallurgy* 66:13-38.
- Lapidus, L. and N.R. Amundson. 1952. Mathematics of adsorption in beds. VI. The effect of longitudinal diffusion in ion exchange and chromatographic columns. *J. Phys. Chem.* 56:984-988.
- Lawes, J.B., J.H. Gilbert and R. Warington. 1881. On the amount and composition of the rain and drainage waters collected at Rothamsted. *J. R. Agr. Soc.* 17 (2nd series):249-279 and 311-350.

- Low, P.F. 1961. Physical chemistry of clay-water interaction. *Advances in Agron.* 13:269-327.
- Luckner, L. and W.M. Schestakow. 1991. *Migration Processes in the Soil and Groundwater Zone.* Lewis Publ. Inc., Chelsea, Michigan.
- Maisel, H. and G. Gnugnoli. 1972. *Simulation of Discrete Stochastic Systems.* Sci. Res. Assoc. Inc., Chicago.
- Mansell, R.S., D.R. Nielsen and D. Kirkham. 1968. A method for simultaneous control of aeration and unsaturated water movement in laboratory soil columns. *Soil Sci.* 106:114-121.
- Marle, C. and P. Defrenne. 1960. La description mathématique du déplacement de fluides miscibles dans un milieu poreux. *Rapp. Inst. Fr. Petrole No.* 5433.
- Marshall, T.J. 1958. A relation between permeability and size distribution of pores. *J. Soil Sci.* 9:1-8.
- Matheron, G. 1965. Regionalized variables and their estimation (in French). Editions Masson, Paris.
- McLaren, A.D. 1970. Temporal and vectorial reactions of nitrogen in soil: A review. *Can. J. Soil Sci.* 50:97-109.
- Means, T.H. and J.G. Holmes. 1901. Soil survey around Fresno, California. *Field Operations of the Division of Soils, 1900.* U.S. Dept. Agr., House of Representatives, Document No. 526. Washington, D.C., p. 333-384.
- Miller, C.W. and L.V. Benson. 1983. Simulation of solute transport in a chemically reactive heterogeneous system: Model development and application. *Water Resour. Res.* 19:381-391.
- Miller, R.J., J.W. Biggar and D.R. Nielsen. 1965. Chloride displacement in Panoche clay loam in relation to water movement and distribution. *Water Resour. Res.* 1:63-73.
- Millington R.J. and J.P. Quirk. 1959. Permeability of porous media. *Nature* 183:387-388.
- Mishra, B.K. and C. Misra. 1993. Nitrogen transformation during miscible displacement of ammonium nitrate solution through the root zone of maize. *J. Indian Soc. Soil Sci.* 41:630-635.
- Misra, C., D.R. Nielsen and J.W. Biggar. 1974. Nitrogen transformations in soil during leaching. I. Theoretical considerations. *Soil Sci. Soc. Am. Proc.* 38:289-293.
- Nerpin, S.V. and A.F. Chudnovskij. 1967. *Soil Physics (in Russian).* Nauka, Moscow.
- Nielsen, D.R. and J.W. Biggar. 1961. Miscible displacement in soils. I. Experimental information. *Soil Sci. Soc. Am. Proc.* 25:1-5.
- Nielsen, D.R. and J.W. Biggar. 1961. Measuring capillary conductivity. *Soil Sci.* 92:192-193.
- Nielsen, D.R., J.W. Biggar and K.T. Erh. 1973. Spatial variability of field measured soil water properties. *Hilgardia* 42:215-259.
- Nielsen, D.R., J.W. Biggar and R.J. Miller. 1967. Field observations of infiltration and soil-water redistribution. *Trans. Am. Soc. Agr. Eng.* 10:382-387.
- Nielsen, D.R., M.T. van Genuchten and J.W. Biggar. 1986. Water flow and solute transport processes in the unsaturated zone. *Water Resour. Res.* 22:895-1085.
- Nkedi-Kizza, P. 1979. Ion exchange in aggregated porous media during miscible displacement. Ph.D. dissertation. Univ. of Calif., Davis.
- Nkedi-Kizza, P., J.W. Biggar, M.Th. van Genuchten, P.J. Wierenga, H.M. Selim, J.M. Davidson and D.R. Nielsen. 1984. On the equivalence of two conceptual models for describing ion exchange during transport through an aggregated oxisol. *Water Resour. Res.* 20:1123-1130.
- Nye, P.H. and P.B. Tinker. 1977. *Solute Movement in the Soil-Root System.* Univ. of Calif. Press, Berkeley.
- Oatmans, H.D. 1962. Nonlinear theory for frontal stability and viscous fingering in porous media. *Soc. Petrol. Engr. J.* 2:165-176.
- Oster, J.D. and H. Frenkel. 1980. The chemistry of the reclamation of sodic soils with gypsum and lime. *Soil Sci. Soc. Am. J.* 44:41-45.
- Othmer, H., B. Diekkrüger and M. Kutflek. 1991. Bimodal porosity and unsaturated hydraulic conductivity. *Soil Sci.* 152:139-150.
- Peck, A.J. 1984. Field variability of soil physical properties. *Adv. in Irrig.* 2:189-221.
- Pfannkuch, H.O. 1962. Contribution à l'étude des déplacements de fluides miscibles dans un milieu poreux. *Revue de l'Institut Français du Pétrole* 18:215-270.
- Reardon, E.J. 1981.  $K_d$ 's - Can they be used to describe reversible ion sorption reactions in contaminant migration?. *Ground Water* 19:279-286.
- Rible, J.M. and L.E. Davis. 1955. Ion exchange in soil columns. *Soil Sci.* 79:41-47.
- Richter, O., P. Nörtesheuser and B. Diekkrüger. 1992. Modeling reactions and movement of organic chemicals in soils by coupling of biological and physical processes. *Modeling Geo-Biosphere Proc.* 1:95-114.
- Robert, P.C., R.H. Rust and W.E. Larson. 1993. *Proceedings of Soil Specific Crop Management: A Workshop on Research and Development Issues.* Special Pub., Am. Soc. Agron., Crop Sci. Soc. Am. and Soil Sci. Soc. Am., Madison, Wisconsin.
- Roth, K. and W.A. Jury. 1993. Modeling the transport of solutes to groundwater using transfer functions. *J. Environ. Qual.* 22:487-493.
- Russo, D. 1993. Stochastic modeling of macrodispersion for solute transport in a heterogeneous unsaturated porous formation. *Water Resour. Res.* 29:383-397.
- Saffman, P.G. 1959. A theory of dispersion in a porous medium. *J. Fluid Mech.* 6:321-349.
- Saffman, P.G. 1960. Dispersion due to molecular diffusion and macroscopic mixing in flow through a network of capillaries. *J. Fluid Mech.* 7:194-208.
- Sallam, A., W.A. Jury and J. Letey. 1984. Measurement of gas diffusion coefficient under relatively low air-filled porosity. *Soil Sci. Soc. Am. J.* 48:3-6.
- Sardin, M., D. Schweich, F.J. Leij and M.Th. van Genuchten. 1991. Modeling the nonequilibrium transport of linearly interacting solutes in porous media: A review. *Water Resour. Res.* 27:2287-2307.
- Scheidegger, A.E. 1954. *Statistical hydrodynamics in porous media.* J. Appl. Phys. 25:994.
- Scheidegger, A.E. 1957. *The Physics of Flow through Porous Media.* Second edition, 1960. Univ. Toronto Press, Toronto.

- Selim, H.M., J.M. Davidson and R.S. Mansell. 1976. Evaluation of a two-site adsorption-desorption model for describing solute transport in soils. Paper presented at Proceedings, Summer Computer Simulation Conference, Nat. Sci. Found., Washington, D.C., July 12-14.
- Shaffer, M.S., R.W. Ribbens, and C.W. Huntley. 1977. Prediction of mineral quality of irrigation return flow, vol. V. Detailed return flow salinity and nutrient simulation model. EPA-600/2-77-179e, U.S. Environ. Prot. Agency, Washington, D.C.
- Simmons, C.S. 1982. A stochastic-convective transport representation of dispersion in one-dimensional porous media systems. *Water Resour. Res.* 18:1193-1214.
- Simpson, E.S. 1969. Velocity and the longitudinal dispersion coefficient in flow through porous media. In: R.J.M. De Wiest (Ed.): *Flow through porous media*, Academic Press, New York and London, p. 201-214.
- Šimůnek, J. and D.L. Suarez. 1994. Two-dimensional transport model for variably saturated porous media with major ion chemistry. *Water Resour. Res.* 30:1115-1133.
- Skopp, J. 1986. Analysis of time-dependent chemical processes in soils. *J. Environ. Qual.* 15:205-213.
- Slichter, C.S. 1905. Field measurements of the rate of movement of underground waters. *Water Supply and Irrigation*, Paper No. 140, Series O, U.S. Dept. Interior, U.S. Geol. Survey, p. 9-122.
- Sposito, G. 1984. *The Surface Chemistry of Soils*. New York, Oxford University Press.
- Sposito, G., V.J. Gupta and R.N. Bhattacharya. 1979. Foundation theories of solute transport in porous media: a critical review. *Advances in Water Res.* 2:59-68.
- Starr, J.L., F.E. Broadbent and D.R. Nielsen. 1974. Nitrogen transformations during continuous leaching. *Soil Sci. Soc. Am. Proc.* 38:283-289.
- Sudicky, E.A., R.A. Gillham and E.O. Frind. 1985. Experimental investigation of solute transport in stratified porous media, 1. The non-reactive case. *Water Resour. Res.* 21:1035-1041.
- Tanji, K.K., L.D. Doneen, G.V. Ferry and R.S. Ayers. 1972. Computer simulation analysis on reclamation of salt-affected soil in San Joaquin Valley, California. *Soil Sci. Soc. Am. Proc.* 36:127-133.
- Taylor, G.I. 1953. Dispersion of soluble matter in solvent flowing slowly through a tube. *Proc. Roy. Soc. London A.* 219:186-203.
- Taylor, S.A. and G.L. Ashcroft. 1972. *Physical Edaphology*. W. H. Freeman and Co. San Francisco.
- Thomas, H.C. 1944. Heterogeneous ion exchange in a flowing system. *J. Am. Chem. Soc.* 66:1664-1666.
- Travis, C.C. and E.C. Etnier. 1981. A survey of sorption relationships for reactive solutes in soil. *J. Environ. Qual.* 10:219-225.
- Uehara, G., B.B. Trangmar and R.S. Yost. 1985. Spatial variability of soil parameters. In D.R. Nielsen and J. Bouma (eds.) *Soil Spatial Variability*. Pudoc, Wageningen, The Netherlands, p. 61-95.
- Valocchi, A.J. 1984. Describing the transport of ion-exchanging contaminants using an effective  $K_d$  approach. *Water Resour. Res.* 20:499-503.
- Van der Molen, W.H. 1956. Desalinization of soils as a column process. *Soil Sci.* 81:19-27.
- van Genuchten, M.Th. 1985. A general approach for modeling solute transport in structured soils. *Memoires Intl. Assoc. Hydrogeol.* 17:513-526.
- van Genuchten, M.Th. and W.J. Alves. 1982. Analytic solutions of the one-dimensional convective-dispersive solute transport equation. *Tech. Bull.* 1661, U.S. Dept. of Agr., Washington, D.C.
- van Genuchten, M.Th. and P.J. Wierenga. 1976. Mass transfer studies in sorbing porous media. I. Analytical solutions. *Soil Sci. Soc. Am. J.* 40:473-480.
- van Genuchten, M.Th., J.M. Davidson and P.J. Wierenga. 1974. An evaluation of kinetic and equilibrium equations for the prediction of pesticide movement in porous media. *Soil Sci. Soc. Am. Proc.* 38:29-35.
- Vauclin, M., S.R. Vieira, G. Vachaud and D.R. Nielsen. 1983. The use of cokriging with limited field soil observations. *Soil Sci. Soc. Am. J.* 47:175-184.
- Wagenet, R.J. and J.L. Starr. 1977. A method for simultaneous control of the water regime and gaseous atmosphere in soil columns. *Soil Sci. Soc. Am. J.* 41:658-659.
- Wagenet, R.J., J.W. Biggar and D.R. Nielsen. 1977. Tracing the transformations of urea fertilizer during leaching. *Soil Sci. Soc. Am. J.* 41:896-902.
- Wang, J.H. 1952. Tracer-diffusion in liquids. III. The self-diffusion of chloride ion in aqueous sodium chloride solutions. *J. Am. Chem. Soc.* 74:1612-1615.
- Webster, R. 1985. Quantitative spatial analysis of soil in the field. *Advances in Soil Sci.* Vol. 3:1-70. Springer Verlag, New York.
- Webster, R. and M.A. Oliver. 1990. *Statistical Methods in Soil and Land Resource Survey*. Oxford Univ. Press.
- Wheatcraft, S.W. and J.H. Cushman. 1991. Hierarchical approaches to transport in heterogeneous porous media. *Rev. Geophys.* 29 Supplement:261-267.
- Wilding, L.P. 1985. Spatial variability: its documentation, accommodation and implication to soil surveys. In: D.R. Nielsen and J. Bouma (Eds.): *Soil Spatial Variability*. Pudoc, Wageningen.
- Wilson, J.N. 1940. A theory of chromatography. *J. Am. Chem. Soc.* 63:1583-1591.
- Wooding, R.A. 1959. The stability of a viscous liquid in a vertical tube containing porous material. *Proc. Roy. Soc. London A.* 252:120-134.
- Yeh, G.T. and S.V. Tripathi. 1991. A model for simulating transport of reactive multispecies components: Model development and demonstration. *Water Resour. Res.* 27:3075-3091.
- Yeh, T.-C., L.W. Gelhar and A.L. Gutjahr. 1985a. Stochastic analysis of unsaturated flow in heterogeneous soils, 1. Statistically anisotropic media with variable  $\alpha$ . *Water Resour. Res.* 21:447-456.
- Yeh, T.-C., L.W. Gelhar and A.L. Gutjahr. 1985b. Stochastic analysis of unsaturated flow in heterogeneous soils, 2. Statistically isotropic media. *Water Resour. Res.* 21:457-464.
- Yeh, T.-C., L.W. Gelhar and A.L. Gutjahr. 1985c. Stochastic analysis of unsaturated flow in heterogeneous soils, 3. Observations and applications. *Water Resour. Res.* 21:465-472.